J. Phys. B: At. Mol. Phys. 19 (1986) 929-968. Printed in Great Britain

Elastic scattering and excitation of the 1s→2s and 1s→2p transitions in atomic hydrogen by electrons at medium to high energies

W L van Wyngaarden† and H R J Walters

Department of Applied Mathematics and Theoretical Physics, The Queen's University of Belfast, Belfast BT7 1NN, Northern Ireland

Received 11 July 1985

Abstract. Multi-pseudostate close coupling is used to investigate 1s→1s, 1s→2s and 1s→2p scattering at energies from 54.4 to 350 eV. Two sets of pseudostates are considered. The first is that of Fon *et al*; the second is an improved set. In constructing the improved pseudostates emphasis is placed upon getting the second Born term right. Target states of angular symmetries not included in the pseudostate bases are taken into account by using the distorted-wave second Born approximation of Kingston and Walters. Results for elastic scattering are satisfactory; it is estimated that the present elastic differential cross sections are accurate to better than 5% at any angle at 200 and 300 eV. For the 2s and 2p excitations the theoretical picture is not so clear. Here there are significant differences between our results and the experiments of Williams and of Williams and Willis. Some other theoretical calculations are in better accord with these experiments, although we believe the present work to be on firmer ground. Cases where the theoretical approximations are unanimously in disagreement with experiment suggest the presence of inaccuracies in the measurements and highlight the need for further experimental investigation. Of special interest are the angular correlation parameters for the 1s→2p excitation; our results are in reasonable agreement with the main experiment at 54.4 eV in the angular range up to 70°; beyond 70° there are still problems to be resolved.

1. Introduction

At medium to high energies the importance ensuring that an approximation is correct at the second Born level is well established (Walters 1984). Elastic scattering methods which take care of the treatment of the second Born term have been very successful, for example, the distorted-wave second Born approximation (Dewangan and Walters 1977, Kingston and Walters 1980), the eikonal-Born series (Byron and Joachain 1973, 1977), the unitarised eikonal-Born series (Byron *et al* 1981, 1982, 1985), the second-order potential method (Winters *et al* 1974, Scott and Bransden 1981, Bransden *et al* 1982). However, for excitation the agreement with experiment has not been so good, particularly in the case of atomic hydrogen (Byron and Latour 1976, Kingston and Walters 1980, 1982, Bransden *et al* 1982). Worse still the 'second-order theories' have been significantly at odds with one another.

† Permanent address: Physics Department, California Polytechnic State University, San Luis Obispo, California 93407, USA.

0022-3700/86/060929+40$02.50

When Kingston and Walters (1980) produced their distorted-wave second Born approximation (DWSBA) cross sections for the 1s → 2s and 1s → 2p transitions in hydrogen they were very surprised to find that, when compared with experiment, their results were inferior to those of much simpler approximations such as three-state 1s-2s-2p close coupling (CC3) (Kingston *et al* 1976). The situation is illustrated in figure 1 where the DWSBA and CC3 numbers are compared with the experiment of Williams and Willis (1975) at 100 eV. The CC3 cross section in this figure is in poor accord with experiment; yet if we now employ the DWSBA, which should be a better approximation, instead of getting improvement towards the experimental results we find divergence away from them!

A further shock awaited the protagonists of the DWSBA. At that time there were two other calculations on atomic hydrogen also based upon second Born ideas: the eikonal-Born series (EBS) of Byron and Latour (1976) and the modified Glauber approximation (MGA) of Gien (1979). These approximations are also shown in figure 1. Here, in both cases, there is improved agreement with experiment, compared with CC3. Thus the predictions of the EBS and MGA are substantially in disagreement with the DWSBA.

In this paper we shall show that it is the trend predicted by the DWSBA which is correct and not that of the EBS and MGA approximations, even though the latter are supported by the experiment.

What is wrong with the EBS approximation of Byron and Latour (1976) is now well understood (Walters 1984). For the 1s → 2p excitation the EBS calculation is really just a form of third Born approximation; for the 1s-2s transition it is a little better (see

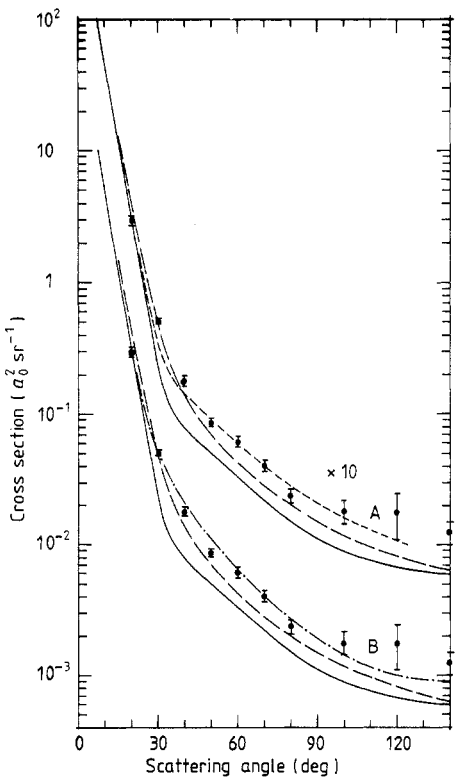

Figure 1. Differential cross sections for $e^- + H(1s) \rightarrow e^- + H(2s+2p)$ at 100 eV. The DWSBA of Kingston and Walters (1980) (——), the 1s-2s-2p close-coupling approximation of Kingston *et al* (1976) (— —) and the experimental data of Williams and Willis (1975) (●) are compared with A, the EBS of Byron and Latour (1976) (- - - -) and B, the MGA of Gien (1979) (— · —). The experimental error bars correspond to two standard deviations.

Byron and Latour 1976). The point is that the convergence of the ordinary Born series at large momentum transfers (i.e., large angles) is slow, especially for excitations. This is confirmed by the recent unitarised eikonal-Born series (UEBS) calculations of Byron *et al* (1985) (see figure 12(*a*) of this paper, curve B) which demonstrate that the large angle EBS cross section of figure 1 is too large; further, these UEBS results agree quite well with the DWSBA cross section of figure 1.

The work of Gien has been criticised for the use of a rather drastic closure approximation in the evaluation of the second Born terms (Byron *et al* 1981, Walters 1984). We incline to the view that this leads to spurious agreement with the data of Williams and Willis (1975); of course, it is impossible to be absolutely certain of this diagnosis without recalculating Gien's numbers using a more accurate closure approximation. However, other evidence against the cross sections of Gien is provided by the UEBS calculations mentioned above which support the DWSBA cross section of figure 1; as discussed by Walters (1984), the UEBS approximation should be an improvement upon the MGA.

In this paper we use multi-pseudostate close coupling. Unlike the DWSBA, the second-order potential method (SOPM) (Bransden *et al* 1982) or the recent exact second-order theory (ESOT) of Madison *et al* (1985), this has the advantage of being a non-perturbative approach†; neither does it rely upon Glauber or Wallace approximations to the scattering equations as the MGA and UEBS methods do, i.e., given the pseudostates the coupled scattering equations are solved exactly. However, all approximations have their weaknesses and in the case of pseudostate close coupling it is the question of how to choose the pseudostates. At the start of this section we emphasised the importance of getting the approximation right at the second Born level. This is the guide to the pseudostates; our choice should be such as to give a good representation of the second Born term—an idea suggested earlier, in a slightly different context, by Bransden and Dewangan (1979).

There are only three other pseudostate calculations on atomic hydrogen in the energy range of interest to us (54.4–350 eV) and all of these are at the lowest energy of 54.4 eV. Thus Callaway *et al* (1976) employed pseudostate close coupling but only for total angular momenta less than or equal to three; at higher angular momenta other approximations were used. Morgan (1982) and Edmunds *et al* (1983) took the approach to larger angular momenta but totally neglected exchange. In the present work exchange is properly accounted for and the pseudostate calculation is continued to as high an angular momentum as is necessary, second Born techniques then being used to extrapolate the partial wave series accurately to infinity. A novel feature of the present work is the addition of a correction term to allow for the contributions from the target states of symmetries (i.e., angular momenta) not included in the pseudostate set; this term is calculated perturbatively in the distorted-wave second Born approximation.

In § 2 we outline the plan of our calculations, discuss the choice of pseudostates and describe the approximations used. Section 3 presents the results; here we discuss our different levels of approximation and then make a wide-ranging comparison of our best results with experiment and with other sophisticated theoretical work of recent years; in studying the $n=1$ to $n=2$ excitations the earlier three-state 1s–2s–2p close-coupling calculation (CC3) of Kingston *et al* (1976) provides a useful point of reference. Our conclusions are stated in § 4. Throughout this paper atomic units, in which $\hbar = m_e = e = 1$, are used; the symbol a_0 denotes the Bohr radius.

† See later and § 2.3 for qualifications, however.

2. Theory

2.1. Plan

Our plan is as follows:

(i) to start with some reasonable set of pseudostates;

(ii) to 'improve' upon this set and see how much difference this makes;

(iii) finally to add on the contribution from the target states of symmetries (i.e., angular momenta) not included in the pseudostate set.

Our starting point is the nine-state set of Fon *et al* (1981); this is listed in table 1. The pseudostates in this set have been constructed to have a range similar to the

Table 1. The nine-member pseudostate set of Fon *et al* (1981).

(*a*) States and energies

s states		p states		d states	
State[a]	Energy (au)	State	Energy (au)	State	Energy (au)
1s	−0.5	—	—	—	—
2s	−0.125	2p	−0.125	—	—
$\overline{3s}$	0.0	$\overline{3p}$	0.0	$\overline{3d}$	0.0
$\overline{4s}$	0.75592	$\overline{4p}$	0.52546	$\overline{4d}$	0.47268

(*b*) Pseudostate[b] basis functions (see (4))

s states		p states		d states	
p_i	α_i	p_i	α_i	p_i	α_i
0	0.6981	1	0.753	2	0.9187
1	0.6981	2	0.753	3	0.9187
2	0.6981	3	0.753		
3	0.6981				

[a] Pseudostates are denoted by a bar, eigenstates are unbarred.

[b] These bases apply only to the pseudostates; the eigenstates have their usual forms.

$n = 2$ eigenstates and to reproduce the correct dipole polarisability of the 1s ground state. Note that only s, p and d symmetries appear in table 1. Before going on to more complicated pseudostates it is important to see how well a relatively simple set like this performs.

In 'improving' upon the Fon *et al* set we still restrict ourselves to s, p and d states. The aim in the construction of the improved set is to get a good representation of the s, p and d intermediate-state contributions to the second Born term.

Since the chosen pseudostates are only of s, p and d types, some allowance has yet to be made for the effect of target states of higher angular momenta. For the transitions studied here these higher angular momentum effects are not big (see §§ 3.1.1 and 3.2.1) and might therefore be reasonably estimated in a perturbative manner through the distorted-wave second Born approximation (DWSBA); this, at any rate, is

what we have assumed. It should be noted that in using the DWSBA in this way we ensure that the second Born term is fully calculated in that intermediate target states of all angular momenta contribute to it.

2.2. *Choice of pseudostates*

We write the orthonormal atomic eigenstates of hydrogen (both bound and continuum) as ψ_n. If H_a is the atomic Hamiltonian then

$$H_a\psi_n = \varepsilon_n\psi_n \tag{1}$$

where ε_n is the eigenenergy. We denote the elements of a pseudostate set by $\bar{\psi}_n$, even though some of the elements will be atomic eigenstates. Like the eigenstates, the pseudostates are given the form

$$\bar{\psi}(\boldsymbol{r}) = \bar{R}(r)\,Y_{lm}(\hat{\boldsymbol{r}}) \tag{2}$$

where $\bar{R}(r)$ is the radial part and Y_{lm} is a spherical harmonic in the angular variable $\hat{\boldsymbol{r}}$. The radial functions are normalised so that

$$\int_0^\infty \bar{R}^2(r)r^2\,\mathrm{d}r = 1 \tag{3}$$

and are expanded in a basis of Slater-type orbitals:

$$\bar{R}(r) = \sum_i c_i r^{p_i}\exp(-\alpha_i r). \tag{4}$$

The pseudostate sets are constructed so as to be orthonormal and to diagonalise the atomic Hamiltonian:

$$\langle\bar{\psi}_n|H_a|\bar{\psi}_m\rangle = \bar{\varepsilon}_n\delta_{nm} \tag{5}$$

where $\bar{\varepsilon}_n$ will be called the pseudostate energy. The set of Fon *et al* (1981) is given in table 1 and the improved set in table 2. It will be seen from these tables that the only eigenstates are 1s, 2s, 2p. In testing these sets we are interested not in the eigenstates but in the pseudostates; we shall therefore eliminate the eigenstates from such considerations (see (8)).

As indicated in § 2.1 we shall judge our pseudostates by how well they perform at the second Born level. We must therefore look first at the second Born term.

The plane-wave second Born term for the transition $\psi_0 \to \psi_f$ may be written

$$f_{f0}^{B2}(\boldsymbol{k}_f, \boldsymbol{k}_0) = \sum_n f_{f0}^{B2;n} \tag{6a}$$

where

$$f_{f0}^{B2;n}(\boldsymbol{k}_f, \boldsymbol{k}_0) = -\frac{1}{8\pi^4}\lim_{\eta\to 0+}\int \mathrm{d}\boldsymbol{k}\langle\boldsymbol{k}_f, \psi_f|V|\boldsymbol{k}, \psi_n\rangle\frac{\langle\boldsymbol{k}, \psi_n|V|\boldsymbol{k}_0, \psi_0\rangle}{k_n^2 - k^2 + \mathrm{i}\eta} \tag{6b}$$

$$k_n^2 = k_0^2 + 2(\varepsilon_0 - \varepsilon_n). \tag{6c}$$

Table 2. The improved pseudostate set of the present paper.

(*a*) States and energies

s states		p states		d states	
State[a]	Energy (au)	State	Energy (au)	State	Energy (au)
1s	−0.5	—	—	—	—
2s	−0.125	2p	−0.125	—	—
$\overline{3s}$	−0.0165	$\overline{3p}$	−0.0194	$\overline{3d}$	0.0261
$\overline{4s}$	0.2375	$\overline{4p}$	0.2131	$\overline{4d}$	0.3912
$\overline{5s}$	0.9075	$\overline{5p}$	0.8115	$\overline{5d}$	1.1767
$\overline{6s}$	2.7186	$\overline{6p}$	2.6081	$\overline{6d}$	2.8074
$\overline{7s}$	8.5901	$\overline{7p}$	8.2548	$\overline{7d}$	6.4890
$\overline{8s}$	43.1132	$\overline{8p}$	15.7833	$\overline{8d}$	15.6264

(*b*) Pseudostate[b] basis functions (see (4))

s states		p states		d states	
p_i	α_i	p_i	α_i	p_i	α_i
0	0.7	1	0.7	2	1.25
1	0.7	2	0.7	3	2.05
2	0.7	3	1.205	4	2.05
1	1.5	2	1.5	5	2.735
2	1.5	4	1.61	3	3.80
3	1.5	2	3.0	4	3.80
1	3.0	3	3.46		
2	3.0				

[a] Pseudostates are denoted by a bar, eigenstates are unbarred.
[b] These bases apply only to the pseudostates; the eigenstates have their usual forms.

In (6) the incident electron has momentum $\boldsymbol{k}_0$, the scattered electron momentum $\boldsymbol{k}_f$, and

$$\langle \boldsymbol{k}, \psi | V | k', \psi' \rangle \equiv \int \exp(-i\boldsymbol{k}\cdot\boldsymbol{r}_1)\psi^*(\boldsymbol{r}_2)\left(-\frac{1}{r_1}+\frac{1}{|\boldsymbol{r}_1-\boldsymbol{r}_2|}\right)\exp(i\boldsymbol{k}'\cdot\boldsymbol{r}_1)\psi'(\boldsymbol{r}_2)\,d\boldsymbol{r}_1\,d\boldsymbol{r}_2 \qquad (7)$$

where * represents complex conjugation. The sum on n in (6a) is over all target eigenstates. However, for present purposes we are concerned only with that part of (6a) which comes from states other than 1s, 2s and 2p (see previous paragraph). We therefore define

$$\bar{f}_{f0}^{B2}(\boldsymbol{k}_f, \boldsymbol{k}_0) = \sum_{n\neq 1s,2s,2p} f_{f0}^{B2;n}. \qquad (8)$$

Further, we want to study the contributions to (8) from states of given angular symmetry; we therefore write

$$\bar{f}_{f0}^{B2}(\boldsymbol{k}_f, \boldsymbol{k}_0) = \sum_{l_T=0}^{\infty} \bar{f}_{f0}^{B2}(\boldsymbol{k}_f, \boldsymbol{k}_0, l_T) \qquad (9a)$$

$$\bar{f}_{f0}^{B2}(\boldsymbol{k}_f, \boldsymbol{k}_0, l_T) \equiv \sum_{n(l_T)} f_{f0}^{B2;n} \qquad n(l_T)\neq 1s, 2s, 2p \qquad (9b)$$

where $\Sigma_{n(l_T)}$ means a sum only over target states with angular momentum l_T.

There are two aspects to the sum in (8) and (9*b*). The first is the completeness of the eigenstates:

$$\sum_n |\psi_n\rangle\langle\psi_n| = 1. \tag{10}$$

The second is the influence of the eigenstate energies, through ε_n in (6*c*). In a closure approximation the completeness property is retained at the expense of sacrificing the energies; thus in a closure approximation to (8) and (9*b*) the eigenstates in the sum are given an average energy $\bar{\varepsilon}$ in (6*c*), i.e.,

$$k_n^2 \to \bar{k}^2 = k_0^2 + 2(\varepsilon_0 - \bar{\varepsilon}) \tag{11}$$

the completeness property (10) then being used to perform the sum.

Alternatively we might consider evaluating $\bar{f}_{f0}^{B2}$ by using a pseudostate basis $\bar{\psi}_n$. Assuming that the pseudostates are orthonormalised and diagonalising the atomic Hamiltonian (see (5)), we would approximate $\bar{f}_{f0}^{B2}$ by

$$\bar{f}_{f0}^{B2}(\boldsymbol{k}_f, \boldsymbol{k}_0, l_T) = \sum_{n(l_T)} f_{f0}^{B2;n}(\text{PS}) \qquad n(l_T) \neq 1s, 2s, 2p \tag{12}$$

where the sum is now over those pseudostates with angular momentum l_T and where $f_{f0}^{B2;n}(\text{PS})$ is the same as in (6*b*) but with ψ_n replaced by the pseudostate $\bar{\psi}_n$ and ε_n in (6*c*) replaced by the corresponding pseudostate energy $\bar{\varepsilon}_n$. In the pseudostate amplitude (12) more attention is paid to energy differences than in the closure approximation but at the price of losing completeness, i.e.,

$$\sum_n |\bar{\psi}_n\rangle\langle\bar{\psi}_n| \neq 1 \tag{13}$$

for a finite set of pseudostates.

What really matters, however, is not full completeness but rather 'effective completeness' as far as the second Born term is concerned (Walters 1981). We may test the effective completeness of the pseudostate set by putting all the energies $\bar{\varepsilon}_n$ in $f_{f0}^{B2;n}(\text{PS})$ equal to some reasonable average $\bar{\varepsilon}$. Then (12) differs from the closure approximation to $\bar{f}_{f0}^{B2}(\boldsymbol{k}_f, \boldsymbol{k}_0, l_T)$, with the same average energy $\bar{\varepsilon}$, only in that an incomplete set of pseudostates (13) is used in place of the complete set of eigenstates (10). By comparing the average energy pseudostate approximation with the corresponding closure amplitude we therefore test the importance of the lack of completeness (13) to the second Born term, i.e., we see how 'effectively complete' the pseudostate set is.

We illustrate the above approach for the Fon *et al* pseudostates in table 3(*a*). Here $\bar{f}_{f0}^{B2}(\boldsymbol{k}_f, \boldsymbol{k}_0, l_T)$ is displayed in partial-wave form for $1s \to 1s$ and $1s \to 2s$ scattering at 100 eV. The partial waves $\bar{f}_{f0,l}^{B2}(l_T)$ are defined according to

$$\bar{f}_{f0}^{B2}(\boldsymbol{k}_f, \boldsymbol{k}_0, l_T) = \sum_{l=0}^{\infty} \frac{1}{(k_0 k_f)^{1/2}} \frac{(2l+1)}{2} \bar{f}_{f0,l}^{B2}(l_T) P_l(\hat{\boldsymbol{k}}_0 \cdot \hat{\boldsymbol{k}}_f) \tag{14}$$

For each transition and for each value of l and l_T three partial waves are shown:

(i) one calculated from the Fon *et al* pseudostates; $\overline{3s}$ and $\overline{4s}$ for $l_T = 0$, $\overline{3p}$ and $\overline{4p}$ for $l_T = 1$; $\overline{3d}$ and $\overline{4d}$ for $l_T = 2$;

(ii) one calculated from the improved set of pseudostates; $\overline{3s}$ to $\overline{8s}$ for $l_T = 0$; $\overline{3p}$ to $\overline{8p}$ for $l_T = 1$; $\overline{3d}$ to $\overline{8d}$ for $l_T = 2$;

(iii) one calculated exactly in the closure approximation.

In all three cases the intermediate states have been given an average energy $\bar{\varepsilon} = +0.0779$ au for $1s \rightarrow 1s$ and $\bar{\varepsilon} = -0.0125$ au for $1s \rightarrow 2s$ (Kingston and Walters 1980)†.

The table shows that the Fon *et al* states give an amplitude which is in excellent agreement with the exact closure answer at $l = 10$‡ but is not so good at $l = 0$. Since close collisions of the incident electron with the atom are associated with low values of l and distant collisions with large l, this means that the Fon *et al* states are defective at short range but are, as far as this test is concerned, satisfactory at large range.

In constructing an improved set of pseudostates we should therefore try to correct this short-range deficiency. To do this we need to include in our basis some tighter functions than those used by Fon *et al* (compare tables 1(*b*) and 2(*b*)). Despite this guidance the choice of an improved pseudostate basis is still somewhat arbitrary. Having selected a basis the pseudostates are formed by orthogonalising to the 1s, 2s and 2p eigenstates and then diagonalising the atomic Hamiltonian (see (5)). We have experimented with several bases and finally decided upon the functions given in table 2. Another of our considerations was to get a reasonable energy distribution for the pseudostates (see table 2). Table 3(*a*) shows that the improved pseudostates give good agreement with the exact closure approximation at both $l = 0$ and $l = 10$, as required; i.e., the improved set is 'effectively complete' at all distances.

By ensuring that the improved pseudostates reproduce the exact closure approximation results we have eliminated the one advantage the closure approximation has over the pseudostate approach. Now giving the pseudostates their correct energies (5) in $f_{f0}^{B2;n}(\text{PS})$ we should obtain a much better approximation to the second Born term $\bar{f}_{f0}^{B2}(\boldsymbol{k}_f, \boldsymbol{k}_0, l_T)$.

It is also of interest to see how the two different pseudostate approximations to $\bar{f}_{f0,l}^{B2}(l_T)$ compare when the pseudostates are given their own energies (5). This is shown in table 3(*b*). The agreement between the two sets of pseudostates at the higher l, i.e., $l = 10$, is not quite as good as that seen in table 3(*a*). This illustrates the (obvious) point that there is more to choosing a pseudostate set than passing the effective completeness test of table 3(*a*), although this is still a very important test; obviously the energy spectrum of the pseudostate set is not unimportant. It is noteworthy that for $1s \rightarrow 1s$ scattering at $l_T = 1$ and $l = 10$ the two sets of pseudostates give the same real part for the second Born term. Since at high l the real part of this term contains the dipole polarisability of the 1s ground state (Walters 1984), this implies that the two sets of pseudostates give the same polarisability as the ground state. As the Fon *et al* set was constructed to give the correct polarisability (see § 2.1) it follows that the improved set also has the right value. It is impossible to say *a priori* how the differences between the two pseudostate sets seen in table 3(*b*) will affect the final $1s \rightarrow 1s$ and $1s \rightarrow 2s$ cross sections; the only way to find out is to calculate with these states, which we do in this paper.

The numbers in brackets after the real part of the improved pseudostate terms in table 3(*b*) are the values obtained whenever the $n = 7$ and 8 pseudostate contributions to the term are omitted. At 100 eV the $n = 7$ and 8 pseudostate channels are closed (see table 2(*a*)) so these states only contribute to the real part of the second Born term. One of the further approximations we shall make in this work is to drop closed

† Note that here, unlike Kingston and Walters, $\bar{\varepsilon} = +0.0779$ is used for *both* the real and imaginary parts of the second Born term in the $1s \rightarrow 1s$ case.

‡ For the s states only $l = 0$ is shown; this is because at $l = 10$ the s state contribution is quite small—the s states are only important at short range.

Table 3. Partial wave second Born terms $\bar{f}^{B2}_{l0,l}(l_T)$ (see (14)) at 100 eV for 1s→1s and 1s→2s scattering. Powers of 10 are denoted by a superscript; R labels the real part and I the imaginary part.

(*a*) Average energy calculations ($\bar{\varepsilon} = +0.0779$ au for 1s→1s, $\bar{\varepsilon} = -0.0125$ au for 1s→2s)

			1s→1s			1s→2s		
l	l_T		Fon *et al*[a]	Exact[b]	Improved[c]	Fon *et al*[a]	Exact[b]	Improved[c]
0	0	R	$+6.5^{-3}$	$+8.5^{-3}$	$+7.7^{-3}$	$+3.3^{-3}$	$+4.1^{-3}$	$+4.0^{-3}$
		I	$+7.6^{-2}$	$+8.4^{-2}$	$+8.3^{-2}$	$+6.4^{-2}$	$+6.8^{-2}$	$+6.8^{-2}$
	1	R	$+2.5^{-2}$	$+3.9^{-2}$	$+3.9^{-2}$	$+7.0^{-3}$	$+1.20^{-2}$	$+1.21^{-2}$
		I	$+3.8^{-3}$	$+1.37^{-2}$	$+1.39^{-2}$	$+4.6^{-3}$	$+8.3^{-3}$	$+8.3^{-3}$
	2	R	$+5.0^{-3}$	$+7.8^{-3}$	$+7.7^{-3}$	-6.9^{-4}	-6.4^{-4}	-6.4^{-4}
		I	$+1.14^{-2}$	$+1.53^{-2}$	$+1.53^{-2}$	-3.5^{-3}	-3.5^{-3}	-3.4^{-3}
10	1	R	$+5.7^{-3}$	$+5.7^{-3}$	$+5.7^{-3}$	$+1.9^{-4}$	$+1.4^{-4}$	$+1.3^{-4}$
		I	$+6.0^{-3}$	$+6.0^{-3}$	$+6.0^{-3}$	$+9.9^{-3}$	$+9.9^{-3}$	$+9.9^{-3}$
	2	R	$+4.3^{-4}$	$+4.4^{-4}$	$+4.4^{-4}$	-3^{-5}	-2^{-5}	-3^{-5}
		I	$+1.83^{-3}$	$+1.84^{-3}$	$+1.85^{-3}$	-1.97^{-3}	-1.94^{-3}	-1.96^{-3}

(*b*) Pseudostates with their own energies $\bar{\varepsilon}_n$

			1s→1s		1s→2s	
l	l_T		Fon *et al*[a]	Improved[c]	Fon *et al*[a]	Improved[c]
0	0	R	$+1.6^{-2}$	$+3.0^{-2}$ (2.8)[d]	$+1.2^{-2}$	$+1.7^{-2}$ (1.6)[d]
		I	$+7.8^{-2}$	$+8.6^{-2}$	$+7.0^{-2}$	$+6.8^{-2}$
	1	R	$+1.80^{-2}$	$+2.33^{-2}$ (2.04)	$+1.7^{-3}$	$+2.9^{-3}$ (1.8)
		I	$+3.9^{-3}$	$+4.8^{-3}$	$+6.0^{-3}$	$+6.0^{-3}$
	2	R	$+7.8^{-3}$	$+1.35^{-2}$ (1.21)	-9.7^{-4}	$+1.4^{-3}$ (9.2^{-4})
		I	$+8.7^{-3}$	$+9.5^{-3}$	-8.9^{-3}	-8.1^{-3}
10	1	R	$+5.4^{-3}$	$+5.4^{-3}$ (5.4)	$+1.5^{-3}$	$+1.2^{-3}$ (1.2)
		I	$+5.6^{-3}$	$+5.7^{-3}$	$+8.6^{-3}$	$+8.8^{-3}$
	2	R	$+7.7^{-4}$	$+7.0^{-4}$ (7.0)	$+5.1^{-4}$	$+3.1^{-4}$ (3.1)
		I	$+1.68^{-3}$	$+1.71^{-3}$	-1.46^{-3}	-1.59^{-3}

[a] Calculated using the pseudostates of Fon *et al* (1981), e.g., for $l_T = 0$, using the $\overline{3s}$ and $\overline{4s}$ states.
[b] Exact values in the closure approximation.
[c] Calculated using the improved pseudostates of table 2, e.g., for $l_T = 0$, using the $\overline{3s}$-$\overline{8s}$ states.
[d] Values of the real part when the $n = 7$ and 8 pseudostate contributions are dropped. Note that since the $n = 7$ and 8 channels are closed at 100 eV (see table 2) these states only contribute to the real part. The same power of ten is implied unless otherwise stated.

channels. The values in brackets therefore indicate what kind of error is likely in such an approximation at 100 eV and at the second Born level. The table shows that the error incurred is relatively small† although not quite as small as we would have liked. Note that at the energies studied in this paper (54.4–350 eV) all of the pseudostate channels of the Fon *et al* set are open, see table 1(*a*).

† We would emphasise again that the imaginary parts in table 3(*b*) are totally unaffected by dropping the $n = 7$ and 8 pseudostates.

Finally we would remark that the closure test shows that the improved pseudostates remain effectively complete at the highest energy considered here, i.e., 350 eV. One last qualification should perhaps be added. In principle we should also test the effective completeness of the pseudostates for the $1s \rightarrow 2p$ transition, which is also studied here. Unfortunately we do not at present possess programs to do this. However, we would be surprised if the improved states did not pass the closure test for the $1s \rightarrow 2p$ excitation.

2.3. Approximations

The plan outlined in § 2.1 has been implemented in its fullest form at the energies of 100, 200 and 300 eV. As indicated, the first step is to calculate the scattering amplitude using the states of Fon *et al* (1981), i.e., to solve the coupled equations

$$(\nabla_1^2 + k_n^2) F_n(\boldsymbol{r}_1) = \sum_m \left(2\left\langle \bar{\psi}_n(\boldsymbol{r}_2) \right| -\frac{1}{r_1} + \frac{1}{|\boldsymbol{r}_1 - \boldsymbol{r}_2|} \left| \bar{\psi}_m(\boldsymbol{r}_2) \right\rangle F_m(\boldsymbol{r}_1) \pm \left\langle \bar{\psi}_n(\boldsymbol{r}_2) \right| -\nabla_1^2 - \nabla_2^2 - \frac{2}{r_1} - \frac{2}{r_2} + \frac{2}{|\boldsymbol{r}_1 - \boldsymbol{r}_2|} - k_0^2 - 2\varepsilon_0 \left| F_m(\boldsymbol{r}_2) \right\rangle \bar{\psi}_m(\boldsymbol{r}_1) \right) \quad (15)$$

where the $\bar{\psi}_n$ are the states of Fon *et al* and where + corresponds to singlet scattering and − to triplet scattering. The equations (15) are solved without further approximation to yield scattering amplitudes

$$f_{f0}^{\pm}(\text{Fon, E}) \quad (16)$$

where 0 and f label the initial and final target states respectively and where + and − indicate whether it is singlet or triplet scattering.

The second step should be the solution of equations (15) this time using the improved pseudostates of table 2. However, here two approximations have been made†. The first involves the treatment of exchange. The full solution of equations (15) with a large basis of pseudostates, such as that given in table 2, is not a simple task. Since exchange is not all that important at 100 eV and above we decided to opt for the following approximation to step two:

$$f_{f0}^{\pm}(\text{Improved, E}) \simeq f_{f0}(\text{Improved, NE}) + (f_{f0}^{\pm}(\text{Fon, E}) - f_{f0}(\text{Fon, NE})) \quad (17)$$

Here $f_{f0}(\text{Improved, NE})$ and $f_{f0}(\text{Fon, NE})$ are the amplitudes extracted from (15) when the exchange term is switched off and when the improved and Fon *et al* pseudostates, respectively, are used. The approximation (17) may be viewed as calculating the direct scattering from the improved pseudostates and combining this with an exchange amplitude given by the Fon *et al* set. The approximation (17) should be good at 100 eV and above.

The second approximation is also made for our own convenience; it is the omission of closed channels from the equations (15). At 100 and 200 eV this means that the $n = 7$ and 8 pseudostates of table 2 are dropped‡. At 300 and 350 eV only the $n = 8$

† There is a third minor approximation. The $\overline{3s}$ and $\overline{3p}$ pseudostates in table 2 are very close in energy. Such small energy differences can give rise to problems in solving the coupled equations (15) in the asymptotic region (Fon *et al* 1981). We therefore decided to make the $\overline{3s}$ and $\overline{3p}$ states degenerate with energy equal to their average −0.0180 au. This average has also been used in the calculations of table 3(*b*).

‡ At 200 eV the $\overline{7s}$ and $\overline{7p}$ channels are closed but the $\overline{7d}$ one is open; in the interests of symmetry we decided to drop the $\overline{7d}$ state also.

states are not used. In § 2.2, table 3(*b*), we provided tentative evidence that such an approximation is probably not very important. By f_{f0}(Improved, NE), as in (17), we therefore mean the amplitude obtained by solving the non-exchange equations corresponding to (15) and where the closed channels have been omitted from these equations. Note that the Fon *et al* states (table 1(*a*)) have no closed channels in the energy range of interest to us, i.e., upwards from 54.4 eV.

The third step of the plan, § 2.1, is the addition to (17) of a term allowing for the contribution of target states of angular momenta (AM) not included in the pseudostate set, this term to be calculated in the distorted-wave second Born approximation (DWSBA):

$$f^{\pm}_{f0}(\text{Best, E}) = f^{\pm}_{f0}(\text{Improved, E}) + f^{\pm}_{f0}(\text{DWSBA, AM} \geqslant 3). \tag{18}$$

The DWSBA amplitude is taken from the work of Kingston and Walters (1980). The extraction of the part corresponding to target states with AM $\geqslant 3$ is readily achieved. For example, consider elastic scattering. Here the full DWSBA amplitude is given as

$$f^{\text{CC}}_{1s,1s}(\boldsymbol{k}_f, \boldsymbol{k}_0; 1s) + \sum_{n \neq 1s} f^{\text{DWSBA};n}_{1s,1s} \tag{19a}$$

$$f^{\text{DWSBA};n}_{1s,1s} = -\frac{1}{8\pi^4} \lim_{\eta \to 0+} \int d\boldsymbol{k} \langle F^{\text{in}}_{1s,1s}, \psi_{1s} | V | \boldsymbol{k}, \psi_n \rangle \frac{\langle \boldsymbol{k}, \psi_n | V | F^{\text{out}}_{1s,1s}, \psi_{1s} \rangle}{k_n^2 - k^2 + i\eta} \tag{19b}$$

(equations (15), (23)-(25) of Kingston and Walters (1980)). In (19) $f^{\text{CC}}_{1s,1s}$ is the static-exchange amplitude and $F^{\text{in,out}}_{1s,1s}$ are distorted waves in the static-exchange field with ingoing (outgoing) scattered waves. States with AM $\geqslant 3$ only contribute to the sum in (19); it is therefore easily seen that

$$f^{\pm}_{1s,1s}(\text{DWSBA, AM} \geqslant 3) = \sum_{\substack{\text{all states } n \\ \text{with AM} \geqslant 3}} f^{\text{DWSBA};n}_{1s,1s}. \tag{20}$$

The 1s → 2s and 1s → 2p cases are similarly handled.

Some points concerning the DWSBA amplitudes of Kingston and Walters (1980) are worth highlighting at this stage. Firstly, these amplitudes have been calculated in the closure approximation. Secondly†, although we have indicated the presence of exchange in $f^{\pm}_{f0}$(DWSBA, AM $\geqslant 3$) by the superscripts ±, in actual fact exchange is only included for elastic scattering, $f = 0 = 1s$, and even here it is unimportant above 100 eV (see Kingston and Walters for details). Thirdly, we require the DWSBA numbers at energies up to 300 eV. However, the DWSBA amplitudes for the 1s → 1s and 1s → 2p transitions have only been exactly evaluated up to 200 eV. For elastic scattering at 300 eV the Dewangan-Walters prescription (Dewangan and Walters 1977, Kingston and Walters 1980) is accurate and so can be used to generate the 1s → 1s amplitude. For 1s → 2p at 300 eV we have had to estimate the DWSBA term from its plane-wave counterpart; fortunately, the contribution of $f^{\pm}_{f0}$(DWSBA, AM $\geqslant 3$) to 1s → 2p scattering at 300 eV is small (see § 3.2.1). Finally, it should be remembered that in all cases the contribution from target states with AM $\geqslant 3$ is expected to be relatively small; as a

† Note that the remarks made here apply only to $f^{\pm}_{f0}$ (DWSBA, AM $\geqslant 3$) and not to the *full* DWSBA amplitudes. Exchange is included in all of the full amplitudes and is an important part of them. For example, in elastic scattering the main exchange effect comes through the static-exchange term $f^{\text{CC}}_{1s,1s}$ (see (19*a*)).

result it should not be necessary to make a very accurate calculation of this contribution; it is our feeling that the DWSBA estimate $f^{\pm}_{f0}(\text{DWSBA, AM} \geqslant 3)$ will be adequate.

So much for the calculations at 100, 200 and 300 eV; now let us turn to the two other energies, 54.4 and 350 eV. At 54.4 eV the Fon *et al* pseudostates have been used to calculate $f^{\pm}_{f0}(\text{Fon, E})$ as usual. However, we have not gone on to the second step of employing the improved pseudostates since we judged the approximation (17) and the omission of closed channels implicit in the calculation of $f_{f0}(\text{Improved, NE})$ to be inappropriate at this energy; we have therefore settled for the Fon *et al* pseudostates and proceeded directly to step three i.e., the addition of the DWSBA term. Thus at 54.4 eV our best approximation is

$$f^{\pm}_{f0}(\text{Fon, E}) + f^{\pm}_{f0}(\text{DWSBA, AM} \geqslant 3). \tag{21}$$

At 350 eV steps one and two of the plan have been completed, but since Kingston and Walters (1980) give no DWSBA amplitudes at this energy we have stopped here. Further, at 350 eV our main interest is to compare with the angular correlation data of Back *et al* (1984) at small angles ($<10°$); comparison of our approximations (17) and (18) at 300 eV indicated that the simpler approach (17) should be perfectly adequate for this purpose at 350 eV.

To summarise, therefore, our best approximation at 100, 200 and 300 eV is given by (18). At 54.4 eV the best result is (21), while at 350 eV the best we have done is (17). In the results section (§ 3) we shall refer to these best approximations simply as the *present* work.

2.4. Cross sections and other observables

Given scattering amplitudes, $f^{\pm}_{f0}$, for the transition $\psi_0 \to \psi_f$, where ψ_0 will always be the 1s state here, we calculate the spin-averaged differential cross section, $\sigma(f)$, according to

$$\sigma(f) = \tfrac{1}{4}(k_f/k_0)(|f^{+}_{f0}|^2 + 3|f^{-}_{f0}|^2). \tag{22}$$

By integrating (22) over all scattering angles $d\Omega$ we obtain the corresponding total or integrated cross section for the transition

$$Q_f = \int \sigma(f)\, d\Omega. \tag{23}$$

This should not be confused with the total cross section, Q_T, for electrons incident upon the state ψ_0 which, by the optical theorem, is given by

$$Q_T = \frac{\pi}{k_0} \operatorname{Im}(f^{+}_{00}(\theta = 0) + 3f^{-}_{00}(\theta = 0)) \tag{24}$$

where $f^{\pm}_{00}(\theta = 0)$ is the forward elastic scattering amplitude.

Also of interest to us in the case of the $1s \to 2p$ excitation are the angular correlation parameters (see, e.g., Morgan and McDowell 1975, Kingston *et al* 1982, Slevin 1984)

$$\lambda \equiv \frac{\sigma(2p_0)}{\sigma(2p_0) + 2\sigma(2p_1)} \tag{25}$$

$$R \equiv \frac{\operatorname{Re}\langle f_0^* f_1 \rangle}{\langle |f_0|^2 + 2|f_1|^2 \rangle} \tag{26}$$

$$I \equiv \frac{\mathrm{Im}\langle f_0^* f_1 \rangle}{\langle |f_0|^2 + 2|f_1|^2 \rangle} \tag{27}$$

where the spin average $\langle\ \rangle$ is defined by

$$\langle f_0^* f_1 \rangle \equiv \tfrac{1}{4}(f_0^{+*} f_1^+ + 3 f_0^{-*} f_1^-) \tag{28a}$$

$$\langle |f_0|^2 + 2|f_1|^2 \rangle \equiv \tfrac{1}{4}(|f_0^+|^2 + 2|f_1^+|^2 + 3|f_0^-|^2 + 6|f_1^-|^2). \tag{28b}$$

In the above formulae the $1s \rightarrow 2p_0$ and $1s \rightarrow 2p_{+1}$ amplitudes are denoted simply by subscripts 0 and 1 respectively, * means complex conjugation, and it is assumed that the quantisation axis lies along the incident direction $\boldsymbol{k}_0$; it is also assumed that a factor $e^{-i\phi}$ has been removed from $f_1^{\pm}$ where ϕ is the azimuthal angle of the scattered electron measured about $\boldsymbol{k}_0$ as z axis (see Kingston *et al* 1982).

Another quantity which has been measured in the case of the $1s \rightarrow 2p$ excitation is the polarisation fraction of the Lyman-α radiation, P; this is given in terms of the integrated $2p_0$ and $2p_1$ cross sections by (Percival and Seaton 1958)

$$P = \frac{Q_{2p_0} - Q_{2p_1}}{2.375 Q_{2p_0} + 3.749 Q_{2p_1}}. \tag{29}$$

3. Results

3.1. Elastic scattering

3.1.1. Comparison of approximations. In table 4 the three stages of approximation (16)-(18) are compared at 100 and 300 eV in the case of differential elastic scattering. At 100 eV we see that the differential cross section calculated with the states of Fon *et al* alone, F (i.e., (16)), differs from that calculated in the best approximation, B (i.e., (18)), by at *most* 12% in the angular range 0-50° and 4% in the range 50-180°. The comparison of I (i.e., (17)) with B shows that to get a cross section accurate to better than 7% at any angle at 100 eV we must take account of target states with AM $\geqslant 3$. At 300 eV all three approximations are in agreement to better than 2% at angles greater than 30°.

When integrated elastic cross sections (23) are compared it is found that the one calculated from the Fon *et al* states alone, (16), is 8% smaller than that obtained in the best approximation (18) at 100 eV, and 5% smaller at 300 eV. Both improving the pseudostate set, i.e. (17), and adding on states with AM $\geqslant 3$, i.e. (18), are roughly of equal importance in producing this difference.

As far as the total cross section (24) is concerned it is found that the pure Fon *et al* approximation (16) gives a value 8% lower than the best approximation (18) at 100 eV, and 7% lower at 300 eV. In this case, however, most of the difference arises from including states with AM $\geqslant 3$, i.e., in going from (17) to (18).

In the rest of § 3.1 we shall confine our attention to the best approximation (18) which will be referred to simply as the *present* calculation.

3.1.2. Differential cross sections. Our present cross sections are given in table 5. In figure 2 they are compared with the distorted-wave second Born approximation (DWSBA) of Kingston and Walters (1980) and with the experimental data of Williams (1975) at 100 and 200 eV. There are other experimental data in the energy range of

Table 4. Comparison of approximations (16), (17) and (18)—the maximum percentage change observed in the differential section for elastic scattering.

Energy (eV)	Approximations compared[a]	Angular range (deg)	Maximum change (%)[b]
100	F→I	0–50	7
		50–180	3
	I→B	0–30	7
		30–180	2
	F→B	0–50	12
		50–180	4
300	F→I	0–30	5
		30–180	1
	I→B	0–20	4
		20–180	1
	F→B	0–30	7
		30–180	2

[a] Key: F, states of Fon *et al* (1981) only, i.e. (16); I, improved pseudostates, i.e. (17); B, best approximation (18).
[b] Percentages are relative to the right-hand member of column 2, e.g. in F→I, relative to I.

Table 5. Present differential cross sections for the elastic scattering of electrons by H(1s), in units of $a_0^2\,\mathrm{sr}^{-1}$. Powers of ten are denoted by a superscript.

Angle (deg)	Energy (eV)		
	100	200	300
0	7.55	5.30	4.38
2	5.98	3.53	2.54
4	4.59	2.39	1.68
6	3.53	1.75	1.26
8	2.76	1.35	9.85^{-1}
10	2.20	1.08	7.84^{-1}
14	1.48	7.12^{-1}	4.96^{-1}
20	8.79^{-1}	3.93^{-1}	2.48^{-1}
25	5.91^{-1}	2.41^{-1}	1.41^{-1}
30	4.06^{-1}	1.51^{-1}	8.27^{-2}
35	2.84^{-1}	9.68^{-2}	5.06^{-2}
40	2.01^{-1}	6.39^{-2}	3.23^{-2}
50	1.06^{-1}	3.07^{-2}	1.48^{-2}
60	6.07^{-2}	1.66^{-2}	7.79^{-3}
75	3.06^{-2}	7.87^{-3}	3.62^{-3}
90	1.77^{-2}	4.41^{-3}	2.00^{-3}
110	1.01^{-2}	2.47^{-3}	1.11^{-3}
120	8.26^{-3}	1.98^{-3}	8.82^{-4}
140	6.15^{-3}	1.44^{-3}	6.30^{-4}
160	5.32^{-3}	1.20^{-3}	5.21^{-4}
180	5.07^{-3}	1.14^{-3}	4.88^{-4}

interest to us (Lloyd *et al* 1974, van Wingerden *et al* 1977) but for reasons discussed by Kingston and Walters they are not considered here.

At 100 eV the new cross sections are slightly higher than the DWSBA values at the larger angles. While this puts them in marginally better agreement with experiment the theoretical curve lies still below the experimental points and generally outside the error bars; we would therefore concur with the view of Kingston and Walters that the experimental measurements are too high at this energy.

At 200 eV the DWSBA cross section is indiscernible from the present numbers on the scale of figure 2. Both are roughly in agreement with the experimental data up to about 60° but beyond, in comparison, experiment is too high. Below we shall argue that we now have sufficient confidence in our cross sections to suggest that it is experiment rather than theory which is at fault above 60°.

In table 6 our present numbers are once again compared with experiment and with the DWSBA cross sections. In addition, however, comparison is also made with other recent sophisticated calculations.

The first point to note is the wide variation in the value of the forward cross section; in particular, the forward cross sections of the second-order potential method (SOPM) and of the coupled-channels optical model (CCOM) are much smaller than those given by the present, DWSBA, unitarised eikonal-Born series (UEBS), and third-order optical model (OM3) approximations. These latter four show a fair amount of agreement with each other.

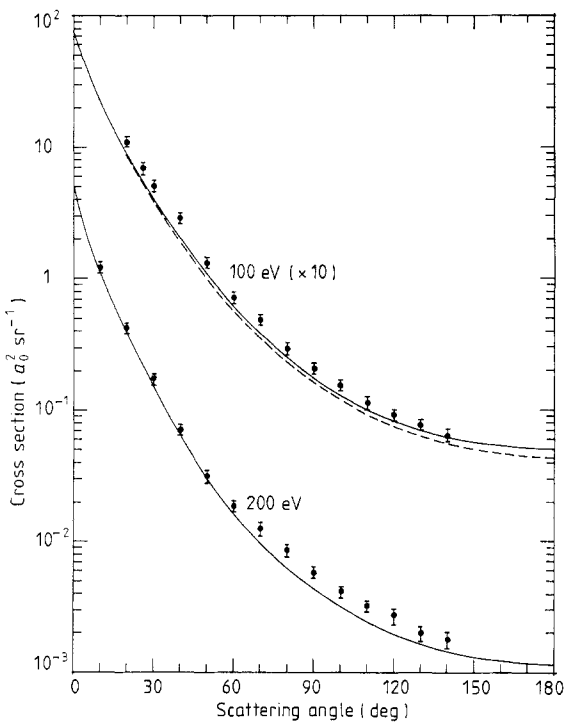

Figure 2. Differential cross sections for elastic $e^- + H(1s)$ scattering at 100 and 200 eV: ——, present results; — —, DWSBA of Kingston and Walters (1980); ●, experimental data of Williams (1975).

One of the difficulties in calculating forward elastic cross sections is to ensure that the long-range polarisation effect is correctly and accurately taken into account. In our experience failure on this point usually leads to a forward cross section which is too small. We would suggest that this is perhaps the explanation of the low forward SOPM and CCOM cross sections seen in table 6.

In the case of the CCOM calculation there is indeed concern about the treatment of polarisation since the local optical potential used in this work does not have the classic leading $-\alpha/2r^4$ polarisation form (McCarthy *et al* 1981). Contrary to claims that have been made (McCarthy *et al* 1982), $-\alpha/2r^4$ is the correct leading long-range behaviour of the exact optical potential for elastic scattering (Walters 1984).

The second point to note from table 6 is the good agreement between all the approximations away from the forward angular region, particularly with increasing energy. At 100 eV all the calculations indicate that the data of Williams (1975) are generally too high. This is also the case at 200 eV and angles beyond 60°. It is this theoretical consensus which gives us the confidence to criticise the experimental measurements.

Table 6. Differential cross sections for the elastic scattering of electrons by H(1s), in units of $a_0^2\,\mathrm{sr}^{-1}$. Powers of ten are denoted by a superscript.

(*a*) 100 eV

Angle (deg)	Expt[a]	Present	DWSBA[b]	UEBS[c]	OM3[d]	SOPM[e]	CCOM[f]
0	—	7.6	7.5	8.2	8.5	4.9	5.8
10	—	2.2	2.2	2.4	2.6	1.9	1.9
20	1.1 (1)	8.8^{-1}	8.5^{-1}	8.5^{-1}	9.0^{-1}	8.0^{-1}	8.6^{-1}
30	5.1^{-1} (5)	4.1^{-1}	3.8^{-1}	3.6^{-1}	3.8^{-1}	3.8^{-1}	4.2^{-1}
40	2.9^{-1} (3)	2.0^{-1}	1.9^{-1}	1.7^{-1}	1.8^{-1}	1.9^{-1}	2.0^{-1}
60	7.2^{-2} (7)	6.1^{-2}	5.6^{-2}	5.3^{-2}	5.4^{-2}	5.9^{-2}	6.3^{-2}
80	3.0^{-2} (3)	2.5^{-2}	2.3^{-2}	2.3^{-2}	2.3^{-2}	2.4^{-2}	2.6^{-2}
100	1.6^{-2} (2)	1.3^{-2}	1.2^{-2}	1.2^{-2}	1.2^{-2}	1.3^{-2}	1.3^{-2}
120	9.2^{-3} (9)	8.3^{-3}	7.6^{-3}	8.0^{-3}	7.5^{-3}	8.2^{-3}	8.0^{-3}
140	6.5^{-3} (7)	6.2^{-3}	5.6^{-3}	5.9^{-3}	5.5^{-3}	6.0^{-3}	5.8^{-3}
160	—	5.3^{-3}	4.6^{-3}	5.0^{-3}	4.6^{-3}	5.0^{-3}	4.8^{-3}
180	—	5.1^{-3}	4.3^{-3}	4.7^{-3}	4.3^{-3}	4.8^{-3}	4.5^{-3}

(*b*) 200 eV

Angle (deg)	Expt[a]	Present	DWSBA[b]	UEBS[c]	OM3[d]	SOPM[e]	CCOM[f]
0	—	5.3	5.2	5.6	5.7	2.9	3.7
10	1.2 (1)	1.1	1.1	1.1	1.1	9.8^{-1}	1.0
20	4.2^{-1} (4)	3.9^{-1}	3.9^{-1}	3.8^{-1}	3.9^{-1}	3.8^{-1}	4.0^{-1}
30	1.7^{-1} (2)	1.5^{-1}	1.5^{-1}	1.5^{-1}	1.5^{-1}	1.5^{-1}	1.5^{-1}
40	7.1^{-2} (7)	6.4^{-2}	6.4^{-2}	6.2^{-2}	6.2^{-2}	6.2^{-2}	6.7^{-2}
60	1.9^{-2} (2)	1.7^{-2}	1.7^{-2}	1.6^{-2}	1.6^{-2}	1.7^{-2}	1.7^{-2}
80	8.6^{-3} (9)	6.3^{-3}	6.3^{-3}	6.4^{-3}	6.3^{-3}	6.5^{-3}	6.7^{-3}
100	4.1^{-3} (4)	3.2^{-3}	3.2^{-3}	3.2^{-3}	3.2^{-3}	3.3^{-3}	3.3^{-3}
120	2.7^{-3} (4)	2.0^{-3}	2.0^{-3}	2.0^{-3}	2.0^{-3}	2.0^{-3}	2.1^{-3}
140	1.8^{-3} (3)	1.4^{-3}	1.4^{-3}	1.4^{-3}	1.4^{-3}	1.4^{-3}	1.5^{-3}
160	—	1.2^{-3}	1.2^{-3}	1.2^{-3}	1.2^{-3}	1.2^{-3}	1.2^{-3}
180	—	1.1^{-3}	1.1^{-3}	1.1^{-3}	1.1^{-3}	1.2^{-3}	1.1^{-3}

Table 6. (continued)

(*c*) 300 eV

Angle (deg)	Present	DWSBA[b]	OM3[d]
0	4.4	4.2	4.5
10	7.8^{-1}	7.5^{-1}	7.9^{-1}
20	2.5^{-1}	2.4^{-1}	2.4^{-1}
30	8.3^{-2}	8.2^{-2}	8.0^{-2}
40	3.2^{-2}	3.2^{-2}	3.2^{-2}
60	7.8^{-3}	7.8^{-3}	7.7^{-3}
80	2.9^{-3}	2.9^{-3}	2.9^{-3}
100	1.5^{-3}	1.5^{-3}	1.5^{-3}
120	8.8^{-4}	8.9^{-4}	8.9^{-4}
140	6.3^{-4}	6.5^{-4}	6.4^{-4}
160	5.2^{-4}	5.4^{-4}	5.3^{-4}
180	4.9^{-4}	5.0^{-4}	5.0^{-4}

[a] Experimental data of Williams (1975). The experimental error in the last figure is given in parentheses.
[b] Distorted-wave second Born approximation of Kingston and Walters (1980).
[c] Unitarised eikonal-Born series of Byron *et al* (1985).
[d] Third-order optical model of Byron and Joachain (1981).
[e] Second-order potential method of Bransden *et al* (1982).
[f] Coupled-channels optical model of McCarthy and Stelbovics (1983a).

Looking at the range of variation of the theoretical numbers in table 6 and, for reasons stated above, discounting the SOPM and CCOM cross sections at forward angles, we would estimate that our present cross sections are probably accurate to better than 5% at any angle at 200 and 300 eV.

The close agreement, and convergence with increasing energy, between the present calculations and DWSBA numbers of Kingston and Walters (1980) confirms the accuracy of the DWSBA for elastic scattering. Beyond 300 eV the DWSBA cross sections are to be recommended.

3.1.3. Integrated elastic cross sections. Table 7 lists integrated elastic cross sections. The experimental values in the table have been obtained by extrapolating and integrating the differential cross sections of Williams (1975). Except for the SOPM cross section at 200 eV, which appears to be a little low, there is agreement between the theoretical numbers within 6%, 4% and 3% respectively at 100, 200 and 300 eV. The experimental value at 200 eV is in reasonable accord with theory but that at 100 eV is too high. This is consistent with the differential cross section comparisons of § 3.1.2.

3.1.4. Total cross sections. In table 8 the various theories are compared with the semi-empirical total cross section estimate of de Heer *et al* (1977). This estimate is considered to have an accuracy of 10%. The present calculation is in excellent agreement with the semi-empirical values. Compared with the DWSBA the present cross section is smaller, the percentage difference between the two increasing as the energy is reduced. This is an encouraging sign since one of the breakdown patterns of the DWSBA is to give a total cross section which becomes too large as the energy is reduced (Dewangan and Walters 1977, Kingston and Walters 1980). It is also noteworthy that

Table 7. Integrated cross sections for the elastic scattering of electrons by H(1s), in units of πa_0^2.

Energy (eV)	Expt[a]	Present	DWSBA[b]	UEBS[c]	OM3[d]	SOPM[e]	CCOM[f]
100	0.588	0.480	0.463	0.465	0.490	0.462	0.465
200	0.204	0.197	0.194	0.196	0.201	0.185	0.194
300	—	0.124	0.121	—	0.124	—	—

[a] As calculated by de Heer *et al* (1977) from the differential measurements of Williams (1975).
[b] Distorted-wave second Born approximation of Kingston and Walters (1980).
[c] Unitarised eikonal-Born series of Byron *et al* (1985).
[d] Third-order optical model of Byron and Joachain (1981).
[e] Second-order potential method of Bransden *et al* (1982).
[f] Coupled-channels optical model of McCarthy and Stelbovics (1983a).

Table 8. Total cross sections, Q_T, for the scattering of electrons by H(1s), in units of πa_0^2.

Energy (eV)	Semi-empirical[a]	Present	DWSBA[b]	UEBS[c]	OM3[d]	SOPM[e]	CCOM[f]
100	2.18	2.13	2.35	2.24	2.44	2.56	2.07
200	1.33	1.31	1.38	1.35	1.39	1.18	1.24
300	0.975	0.961	0.991	—	0.999	—	—

[a] De Heer *et al* (1977).
[b] Distorted-wave second Born approximation of Kingston and Walters (1980).
[c] Unitarised eikonal-Born series of Byron *et al* (1985).
[d] Third-order optical model of Byron and Joachain (1981).
[e] Second-order potential method of Bransden *et al* (1982).
[f] Coupled-channels optical model of McCarthy and Stelbovics (1983a).

the SOPM cross section displays a more drastic fall with energy than the other entries in the table; at 100 eV it gives the largest cross section, at 200 eV the smallest; in both cases it lies beyond the quoted 10% error in the semi-empirical estimate.

3.2. Excitation of the n = 2 states

3.2.1. Comparison of approximations. Table 9 compares the approximations (16)-(18) for the differential cross sections for 1s→2s and 1s→2p excitation at 100 and 300 eV. The percentage changes are on average about a factor of two larger than those of the elastic case (table 4) indicating the greater sensitivity of the excitation cross sections to the precise form of the approximation used. It is clear from table 9 that one must work hard to obtain a cross section accurate to better than 10% at any angle.

The I→B comparison at 300 eV shows that close to the forward direction the 1s→2s cross section receives a significant contribution from target states with AM≥3; the maximum change here of 13% occurs for forward scattering. At 100 eV the maximum change of 14% in the angular range 0-50° also happens in the forward direction. It is well known that important cancellations take place for forward 1s-2s scattering (Kingston and Walters 1980, Buckley and Walters 1975). By contrast the 1s→2p cross section in the forward region, 0-10°, is very insensitive to the form of the approximation; this is because it is dominated by the first Born term.

Table 9. Comparison of approximations (16), (17) and (18)—maximum percentage change observed in differential cross sections for 1s→2s and 1s→2p excitation.

(*a*) 1s→2s excitation

Energy (eV)	Approximations compared[a]	Angular range (deg)	Maximum change (%)[b]
100	F→I	0-40	5
		40-180	20
	I→B	0-50	14
		50-180	4
	F→B	0-180	19
300	F→I	0-180	10
	I→B	0-3	13
		3-180	5
	F→B	0-180	15

(*b*) 1s→2p excitation

Energy (eV)	Approximations compared[a]	Angular range (deg)	Maximum change (%)[b]
100	F→I	0-20	1
		20-120	13
		120-180	20
	I→B	0-10	1
		10-180	13
	F→B	0-10	1
		10-120	16
		120-180	34
300	F→I	0-10	1
		10-180	11
	I→B	0-10	1
		10-180	5
	F→B	0-10	2
		10-40	17
		40-180	8

[a] Key: F, states of Fon *et al* (1981) only, i.e. (16); I, improved pseudostates, i.e. (17); B, best approximation (18).

[b] Percentages are relative to the right-hand member of column 2, e.g. in F→I, relative to I.

At 54.4 eV our best approximation is (21). Comparing this with (16) we find that couplings to target states with AM ≥ 3 change the 1s-2s cross section by up to 18% in the angular region 0-60°, but between 60 and 180° the difference never exceeds 2%. For the 1s→2p excitation changes are less than 2% from 0 to 10° but as much as 16% elsewhere.

Integrated cross sections are insensitive to the form of approximation used. At 100 eV and above the 1s→2s cross sections from approximations (16)-(18) differ by

no more than 3% from one another. There is a little bit more sensitivity at 54.4 eV where the 1s→2s cross section calculated from (21) is 7% larger than that obtained from (16). For the 1s→2p transition all cross sections agree within 1% at 54.4 eV and upwards.

We do not think it worthwhile to detail the differences between approximations (16)-(18) for the angular correlation parameters λ, R and I of (25)-(27). Suffice it to say that there are no substantial variations.

Finally, it should be noted that in the rest of § 3.2 we confine our attention to approximation (18) at 100, 200 and 300 eV, to approximation (21) at 54.4 eV and to approximation (17) at 350 eV (see § 2.3). These we shall refer to as the *present* results.

3.2.2. Results at 54.4 eV. 54.4 eV is special since it is the one energy at which experiment provides differential cross sections for the excitation of the separate 2s and 2p states (Williams 1981). At other energies only the sum, 2s+2p, has been measured. Further, in the energy range of interest here, 54.4 eV is the only energy at which there is a substantial number of experimental data on the angular correlation parameters λ and R.

Differential cross sections for the excitation of the 2s state are shown in figure 3. Here comparison is made between the present calculation, the experimental results of Williams (1981) and other recent theoretical approximations, namely, the distorted-wave second Born approximation (DWSBA) of Kingston and Walters (1980), the 1s-2s-2p close-coupling calculation (CC3) of Kingston *et al* (1976), the second-order potential method (SOPM) of Bransden *et al* (1982), the unitarised eikonal-Born series (UEBS) of Byron *et al* (1985) and the coupled-channels optical model (CCOM) of Bransden *et al* (1984).

When Kingston and Walters (1982) compared their 2s DWSBA cross section with Williams' experiment they were surprised to find so much disagreement. By contrast the simple CC3 calculation of Kingston *et al* (1976), which gave a cross section about twice as large as the DWSBA, was in good accord with the experiment. How could it be that an approximation which attempted to take account of couplings to all target states, the DWSBA, and which showed that such extended coupling was very important, could come off so badly in comparison with an approximation, CC3, which merely coupled three states and ignored the rest? The interesting thing about the present result is that it substantially confirms the DWSBA cross section (see figure 3, curve A), as did the previous non-exchange pseudostate close-coupling calculation of Morgan (1982) using different pseudostates.

Figure 3 (curve B) shows that the UEBS and SOPM approximations, which, like the DWSBA and the present calculation, take account of couplings to all target states, also give cross sections substantially smaller than the CC3 numbers. However, the disturbing thing about these results is that they are also in significant disagreement with the present cross section and with each other.

There is one theory which takes account of coupling to all states and which agrees with the experiment, namely the CCOM calculation of Bransden *et al* (1984). Like the present, DWSBA, UEBS and SOPM approximations this approximation predicts a lower cross section than that obtained from CC3. However, the lowering of the cross section is not so great as in the above mentioned methods; the result is that the CCOM cross section remains in agreement with experiment within the quoted error bars (figure 3, curve C).

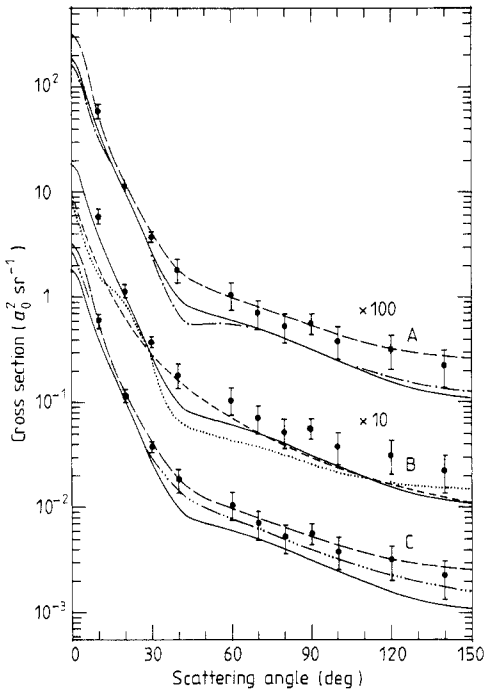

Figure 3. Differential cross sections for $e^- + H(1s) \rightarrow e^- + H(2s)$ at 54.4 eV. The present results (——) and experimental data of Williams (1981) (●) are compared with A, the 1s-2s-2p close-coupling approximation of Kingston *et al* (1976) (— —) and the DWSBA of Kingston and Walters (1980) (— · —), B, the UEBS of Byron *et al* (1985) (- - - -) and the SOPM of Bransden *et al* (1982) (· · · ·), and C, the 1s-2s-2p close-coupling approximation of Kingston *et al* (1976) (— —) and the CCOM of Bransden *et al* (1984) (— · · · —). The experimental error bars correspond to two standard deviations.

Let us look at the CCOM calculation more carefully. In this model coupled equations involving $(M+1)$ eigenstates are solved†:

$$(\nabla_1^2 + k_n^2) F_n(\boldsymbol{r}_1) = 2 \sum_{m=0}^{M} \langle \psi_n | V^{\mathrm{OPT}} | \psi_m \rangle F_m(\boldsymbol{r}_1) \qquad n = 0 \text{ to } m. \tag{30}$$

For the CCOM cross sections shown in figure 3 and elsewhere in this paper n and m run only over the 1s, 2s and 2p states. The matrix elements in (30) are written

$$\langle \psi_n | V^{\mathrm{OPT}} | \psi_m \rangle = \langle \psi_n | V | \psi_m \rangle + \langle \psi_n | \bar{V}^{\mathrm{OPT}} | \psi_m \rangle \tag{31}$$

and a local potential approximation to $\langle \psi_n | \bar{V}^{\mathrm{OPT}} | \psi_n \rangle$ is constructed. Until recently only *diagonal* elements of $\bar{V}^{\mathrm{OPT}}$ had been retained (see McCarthy and Stelbovics (1983b), especially appendix B, and references therein), i.e. the set

$$\langle \psi_n | \bar{V}^{\mathrm{OPT}} | \psi_m \rangle = 0 \qquad n \neq m. \tag{32}$$

Walters (1984) has pointed out that the approximation (32) leads to a scattering amplitude whose second Born term in the case of excitation is simply

$$f_{\mathrm{f0}}^{\mathrm{B2}}(\boldsymbol{k}_{\mathrm{f}}, \boldsymbol{k}_0) = \sum_{n=0}^{M} f_{\mathrm{f0}}^{\mathrm{B2};n} \qquad f \neq 0 \tag{33}$$

i.e., it contains no coupling outside the set ψ_0 to ψ_M. This is exactly the second Born term that would be obtained in a simple $(M+1)$-state close-coupling approximation. Now, it is coupling outside the set 1s, 2s, 2p at the second Born level which is the source of the big difference between the CC3 and DWSBA cross sections of figure 3. We conclude that the CCOM with the approximation (32) will give results which do not

† For simplicity we ignore exchange here. In the CCOM calculations exchange is taken into account.

reflect the true difference from the CC3 values. Later (figures 10–12) we shall note the similarity of the CCOM and CC3 numbers; in these cases the CCOM has been calculated with the approximation (32) (McCarthy and Stelbovics 1983a).

However, the above criticism cannot be levelled at the CCOM cross section of figure 3 (Bransden *et al* 1984). This is the one case in which the approximation (32) has not been made. In their paper Bransden *et al* compare the CCOM numbers with and without the approximation (32); they find relatively little difference between the two. For the 1s–2s excitation we find this very surprising, in view of the work of Kingston and Walters (1980) and of Buckley and Walters (1975) on the analogous $He(1^1S) \rightarrow He(2^1S)$ transition.

It may be, however, that the explanation lies in two other weaknesses of the CCOM calculations. These are: (i) the use of local potentials for both diagonal and non-diagonal elements of $\langle \psi_n | \bar{V}^{OPT} | \psi_m \rangle$; (ii) the procedure used to convert $\langle \psi_n | \bar{V}^{OPT} | \psi_m \rangle$ into a local potential.

Kingston and Walters (1980) have shown that local potential approximations to $\langle \psi_n | \bar{V}^{OPT} | \psi_n \rangle$ can be viable but have cast considerable doubt upon the non-diagonal case $\langle \psi_n | \bar{V}^{OPT} | \psi_m \rangle$ $(m \neq n)$; the example they give is the 1s–2s excitation of hydrogen! Walters (1984) has criticised the particular localisation procedure used in the CCOM calculations, even for diagonal potentials. It is this localisation procedure which gives rise to the spurious long-range behaviour of the CCOM polarisation potential for elastic scattering referred to in § 3.1.2.

Despite the agreement between the CCOM and experiment seen in figures 3–6, we have, for the reasons given above, reservations about the reliability of the CCOM cross sections.

Figure 4 shows the $1s \rightarrow 2p$ cross section at 54.4 eV. The present results are not in particularly good agreement with experiment, although they are marginally better than the DWSBA values. In better accord with experiment are the CC3 and UEBS numbers but, again, the best agreement comes from the CCOM calculation of Bransden *et al* (1984). A new theoretical approximation appearing in figure 4 is the exact second-order theory (ESOT) of Madison *et al* (1985).

The $1s \rightarrow 2s$ cross section of Williams (1981) shown in figure 3 is determined by first measuring the absolute $1s \rightarrow 2p$ cross section (figure 4) and then the ratio, $\sigma(2s)/\sigma(2p)$, of the 2s and 2p cross sections. This measured ratio is shown in figure 5. From this figure we see that only one calculation fully supports the experiment, namely the 1s–2s–2p close-coupling approximation (CC3); this approximation is in agreement with the data within the quoted experimental errors at every point. The CCOM calculation of Bransden *et al* (1984), which agreed so well with the separate 2s and 2p cross sections of figures 3 and 4, is not generally in accord with the measurements of figure 5, although, of the theories shown, it comes second to the CC3 approximation.

Williams (1981) has also independently measured the sum of the 2s and 2p cross sections, $\sigma(2s) + \sigma(2p)$. This is shown in figure 6. The present, DWSBA and SOPM cross sections are not in agreement with experiment; the UEBS results are closer to experiment but not generally in accord; the best support for experiment comes, as expected from figures 3 and 4, from the CC3 and CCOM approximations.

From figures 3–6 it is clear that the theoretical situation at 54.4 eV is confused. Of the calculations exhibited we would have thought that the present approximation is on the firmest ground, yet the resulting cross sections are amongst the worst in giving agreement with experiment. What is needed is an independent remeasuring of the cross sections at this energy; the curves shown in the figures indicate what degree of

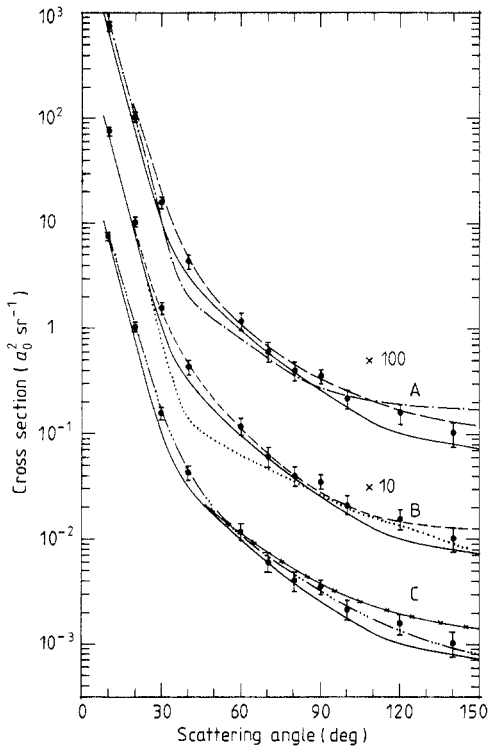

Figure 4. Differential cross sections for $e^- + H(1s) \rightarrow e^- + H(2p)$ at 54.4 eV. The present results (——) and the experimental data of Williams (1981) (●) are compared with A, the 1s-2s-2p close-coupling approximation of Kingston *et al* (1976) (— —) and the DWSBA of Kingston and Walters (1980) (— · —), B, the UEBS of Byron *et al* (1985) (- - - -) and the SOPM of Bransden *et al* (1982) (· · · ·), and C, the ESOT of Madison *et al* (1985) (×-×) and the CCOM of Bransden *et al* (1984) (— · · · —). The experimental error bars correspond to two standard deviations.

accuracy in the measurements will be required to distinguish between the various theoretical predictions.

We turn now to the electron-photon coincidence experiments at 54.4 eV; these provide the two parameters λ and R of (25) and (26). There are three experiments: Williams (1981), Weigold *et al* (1980) and Slevin *et al* (1980). The experiment of Williams covers the same angular range as that of Weigold *et al* but has smaller error bars†. The measurements of Slevin *et al* are confined to a small angular region, 12-20°, near the forward direction. Since there is no significant disagreement between the experiments, we have decided, in the interests of graphical clarity, to compare only with the data of Williams. Again, for the sake of clarity, we consider only the present, CC3, UEBS and ESOT approximations, i.e., we drop the DWSBA, SOPM and CCOM approximations. This is reasonable since the first two do not give very good agreement with the angular correlation data (comparisons may be found in Walters (1984) and Bransden *et al* (1982)), while the CCOM results do not differ greatly from the CC3 values (McCarthy and Stelbovics 1983a, Bransden *et al* 1984).

The λ parameter is shown in figure 7. Three features are worth highlighting: (i) the depth and width of the minimum near 17°; (ii) the maximum near 55°; (iii) the depth of the second minimum at approximately 100°.

The present calculation reproduces well the deep experimental minimum near 17° and also the width of this dip, as indicated by the experimental points at 20, 30 and 40°; in fact, the present results give the best agreement with experiment in this region.

† Note that the errors quoted by Williams (1981) represent two standard deviations. Weigold *et al* (1980) do not specify whether their error estimates are one or two standard deviations. Here we assume it is two, but if it is only one then this means that the data of Williams are of much higher quality.

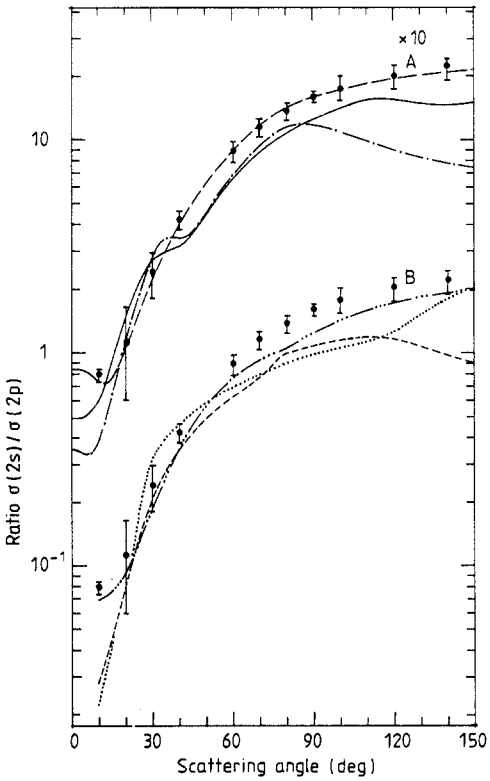

Figure 5. Ratio of 2s and 2p differential cross sections at 54.5 eV. The experimental data of Williams (1981) (●) are compared with A, the present results (——), the 1s-2s-2p close-coupling approximation of Kingston *et al* (1976) (— —) and the DWSBA of Kingston and Walters (1980) (— · —), and B, the UEBS of Byron *et al* (1985) (- - - -), the SOPM of Bransden *et al* (1982) (· · · ·) and the CCOM of Bransden *et al* (1984) (— · · · —). The experimental error bars correspond to two standard deviations.

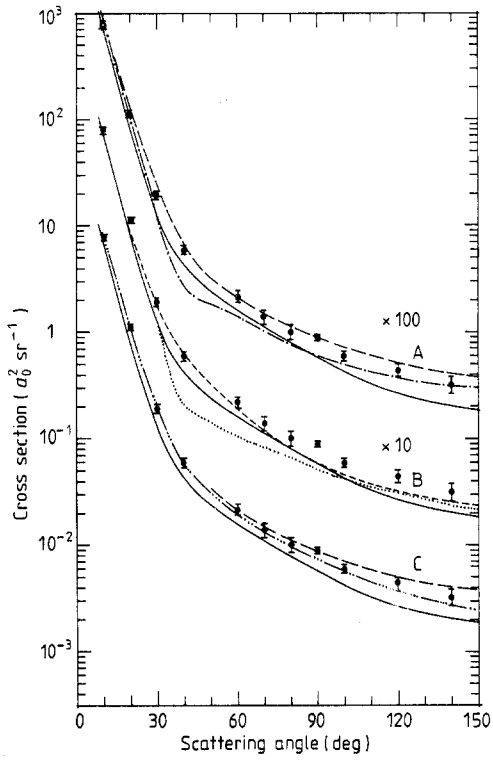

Figure 6. Differential cross sections for e^-+H(1s)→ e^-+H(2s+2p) at 54.4 eV. The present results (——) and the experimental data of Williams (1981) (●) are compared with A, the 1s-2s-2p close-coupling approximation of Kingston *et al* (1976) (— —) and the DWSBA of Kingston and Walters (1980) (— · —), B, the UEBS of Byron *et al* (1985) (- - - -) and the SOPM of Bransden *et al* (1982) (· · · ·), and C, the 1s-2s-2p close-coupling approximation of Kingston *et al* (1976) (— —) and the CCOM of Bransden *et al* (1984) (— · · · —). The experimental error bars correspond to two standard deviations.

The CC3 approximation also gives a sufficiently deep minimum but the dip is too wide. The UEBS approximation fails to give a deep enough plunge. Closest to the present calculation is the ESOT, although it does not quite produce a low enough minimum.

Only the present calculation and the CC3 numbers capture the height of the experimental maximum near 55°. The ESOT is worst in this respect.

The second minimum near 100° is quite interesting. The CC3 approximation gives far too shallow a minimum in this region; the present calculation does better but is still not in agreement with experiment. A deep minimum like that observed in the experiment is given by the UEBS and ESOT approximations. In figure 5(*a*) of their paper Byron *et al* (1985) show the UEBS λ parameter calculated with and without electron exchange. Without exchange a very much deeper minimum occurs at about 95°. On introducing exchange this minimum moves upwards into the rough agreement

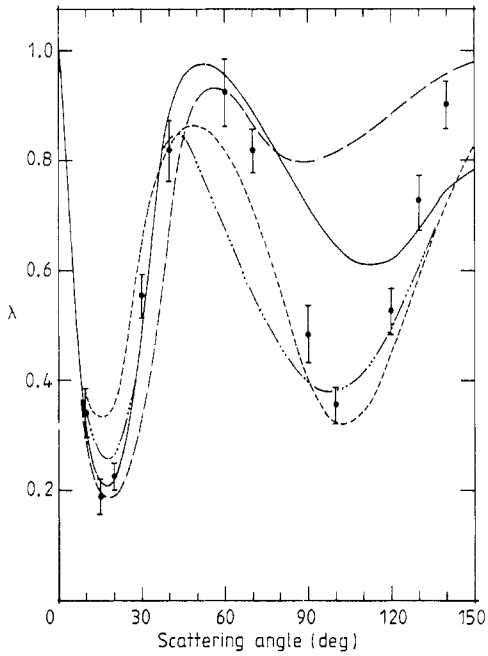

Figure 7. Angular correlation parameter λ at 54.5 eV. ——, present results; — —, 1s-2s-2p close-coupling approximation of Kingston *et al* (1976); - - - -, UEBS of Byron *et al* (1985); — · · · —, ESOT of Madison *et al* (1985); ●, experimental data of Williams (1981). The error bars correspond to two standard deviations.

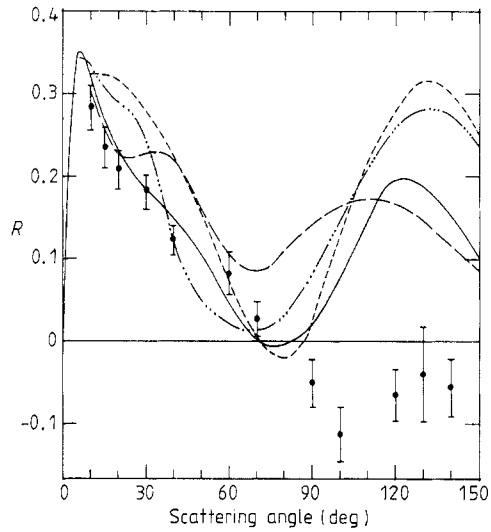

Figure 8. Angular correlation parameter R at 54.4 eV. ——, present results; — —, 1s-2s-2p close-coupling approximation of Kingston *et al* (1976); - - - -, UEBS of Byron *et al* (1985); — · · · —, ESOT of Madison *et al* (1985); ●, experimental data of Williams (1981). The error bars correspond to two standard deviations.

with experiment seen in figure 7. However, Byron *et al* use a relatively crude approximation for the exchange amplitude, namely the first Born exchange term (with the electron-nucleus interaction removed). Since exchange is so important to the UEBS prediction, the viability of this approximation, particularly at an energy as low as 54.4 eV, is a critical factor.

Clearly all of the features of the experimental λ parameter can be explained in some approximation. However, no single theoretical approximation gives agreement with the measurements at all angles.

The R parameter (26) at 54.4 eV is shown in figure 8. The present results reproduce well the trend of the experimental data at angles up to 70°, although only at one point, 30°, is there agreement with experiment within the quoted error bars. The CC3 approximation agrees with experiment up to 20° but then, on developing a shoulder in the region 20-40°, loses contact with the data. The UEBS and ESOT calculations show little accord with the measurements. Beyond 90° all of the theories indicate a rise in the R parameter to a positive maximum. Experiment, on the other hand, gives an almost mirror-image result, i.e., a fall to a negative minimum.

Figure 9 shows the I parameter (27) at 54.4 eV. There are no experimental measurements of this parameter. While all four theories agree on trends there are significant differences on detail.

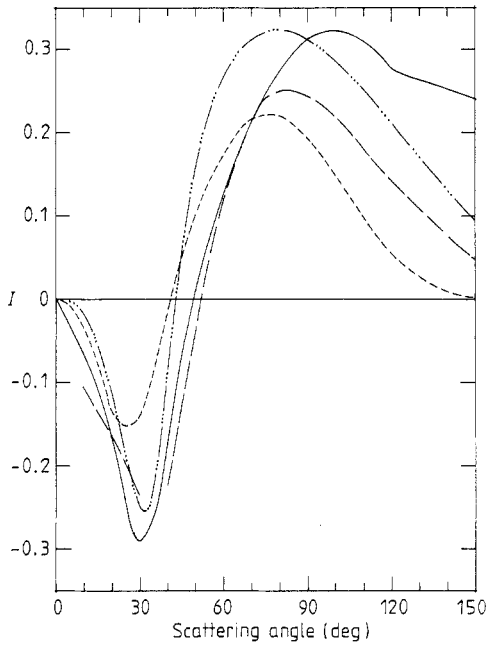

Figure 9. Angular correlation parameter I at 54.5 eV. ——, present results; ——, 1s-2s-2p close-coupling approximation of Kingston *et al* (1976); - - - -, UEBS of Byron *et al* (1985); —···—, ESOT of Madison *et al* (1985).

Looking at figures 7 and 8, and not being too critical, it is fair to say that there is a reasonable amount of agreement between the present calculations and the experimental angular-correlation data in the angular region up to 70°.

3.2.3. Differential cross sections. The present differential cross sections are given in tables 10 and 11. In figures 10, 11 and 12 they are compared with other theoretical work at 100, 200 and 300 eV. It should be noted that the SOPM (Bransden *et al* 1982) and CCOM (McCarthy and Stelbovics 1983a) approximations have only been calculated as far as 200 eV, this explains their absence from figures 10(*c*), 11(*c*) and 12(*c*). Further, the 200 eV SOPM numbers at large angles exhibit an oscillation which is presumably due to numerical inaccuracies in the calculation; it is for this reason that the SOPM cross sections in figures 10(*b*) (curve B), 11(*b*) (curve B) and 12(*b*) (curve B) are not continued to very large angles.

Consider the 1s→2s transition (figure 10). Here, with the exception of CCOM, all of the more sophisticated approximations give a smaller cross section than three-state close coupling (CC3). This statement is also true for CCOM at 100 eV and at the larger angles; however, with increasing energy the CCOM cross section rapidly approaches the CC3 approximation at all angles, so that by 200 eV it is almost indistinguishable from CC3 on the scale of figure 10. This illustrates the point made in the previous section— the approximation (32) will lead to results which are, unrealistically, similar to CC3. By contrast the other theoretical curves in figure 10 are noticeably different from the CC3 numbers right up to 300 eV.

The large disparity between the CC3 and CCOM forward 1s→2s cross sections and the other approximations, even at energies as high as 200 and 300 eV, is very significant. Although there is a large discrepancy between the UEBS and SOPM cross sections, on the one hand, and the present and DWSBA results, on the other hand, at 54.4 eV (figure

Table 10. Present differential cross sections for the 1s→2s excitation of atomic hydrogen by electron impact, in units of $a_0^2\,\mathrm{sr}^{-1}$. Powers of ten are denoted by a superscript.

Angle (deg)	Energy (eV)				
	54.4	100	200	300	350[a]
0	1.85	1.59	1.39	1.39	1.20
2	1.64	1.21	9.51^{-1}	9.24^{-1}	8.65^{-1}
4	1.20	7.81^{-1}	7.10^{-1}	6.66^{-1}	6.27^{-1}
6	8.17^{-1}	5.62^{-1}	5.31^{-1}	4.58^{-1}	4.20^{-1}
8	5.56^{-1}	4.29^{-1}	3.78^{-1}	2.90^{-1}	2.55^{-1}
10	3.93^{-1}	3.29^{-1}	2.54^{-1}	1.69^{-1}	1.40^{-1}
12	2.90^{-1}	2.49^{-1}	1.62^{-1}	9.28^{-2}	7.22^{-2}
14	2.21^{-1}	1.84^{-1}	9.96^{-2}	4.89^{-2}	3.59^{-2}
16	1.71^{-1}	1.34^{-1}	5.97^{-2}	2.55^{-2}	1.79^{-2}
18	1.33^{-1}	9.58^{-2}	3.54^{-2}	1.35^{-2}	9.29^{-3}
20	1.03^{-1}	6.75^{-2}	2.11^{-2}	7.50^{-3}	5.14^{-3}
25	5.32^{-2}	2.74^{-2}	6.83^{-3}	2.39^{-3}	1.66^{-3}
30	2.72^{-2}	1.22^{-2}	3.14^{-3}	1.15^{-3}	7.92^{-4}
35	1.50^{-2}	7.02^{-3}	1.87^{-3}	6.85^{-4}	4.64^{-4}
40	9.97^{-3}	4.93^{-3}	1.24^{-3}	4.40^{-4}	2.89^{-4}
45	8.12^{-3}	3.78^{-3}	8.56^{-4}	2.92^{-4}	1.86^{-4}
50	7.34^{-3}	2.96^{-3}	6.04^{-4}	2.02^{-4}	1.34^{-4}
60	6.28^{-3}	1.80^{-3}	3.22^{-4}	1.02^{-4}	6.30^{-5}
75	4.59^{-3}	8.83^{-4}	1.46^{-4}	4.47^{-5}	2.72^{-5}
90	3.22^{-3}	4.88^{-4}	7.68^{-5}	2.32^{-5}	1.41^{-5}
110	1.99^{-3}	2.82^{-4}	4.09^{-5}	1.21^{-5}	7.4^{-6}
120	1.58^{-3}	2.47^{-4}	3.24^{-5}	9.54^{-6}	—
140	1.18^{-3}	1.95^{-4}	2.30^{-5}	7.10^{-6}	—
160	—	1.83^{-4}	1.92^{-5}	6.35^{-6}	—
180	—	1.76^{-4}	1.68^{-5}	5.87^{-6}	—

[a] Note that the 350 eV numbers have been calculated in approximation (17), while at 100, 200 and 300 eV approximation (18) has been used.

3), by 200 eV there is little difference between these four approximations in the forward angular region. This is in sharp contrast with the CC3 and CCOM results which persist in being very much larger right up to 300 eV. Thus at 100, 200 and 300 eV the present 1s→2s zero-angle cross sections are 1.6, 1.4 and 1.4 $a_0^2\,\mathrm{sr}^{-1}$; this compares with the CC3 values of 3.6, 3.3 and 3.5 $a_0^2\,\mathrm{sr}^{-1}$ respectively and the CCOM values of 3.5 and 3.0 $a_0^2\,\mathrm{sr}^{-1}$ at 100 and 200 eV.

This pronounced difference shows the importance of including couplings to all target states, at least at the second Born level. Thus it is found that second Born couplings to 1s, 2s and 2p intermediate states are partially cancelled by couplings to other intermediate states in the forward angular region; it is this cancellation which leads to the present, DWSBA, UEBS and SOPM cross sections being much lower than the CC3 results at forward angles (see Kingston and Walters 1980, Buckley and Walters 1975). We have earlier explained why the CC3 and CCOM calculations should agree—approximation (32).

Figure 11 compares 1s→2p cross sections at 100, 200 and 300 eV. In the interests of clarity the CC3 cross section at 200 eV is not shown; it should come as no surprise that it lies close to the CCOM values.

Table 11. Present differential cross sections for the 1s→2p excitation of atomic hydrogen by electron impact, in units of $a_0^2\,sr^{-1}$. Powers of ten are denoted by a superscript.

Angle (deg)	Energy (eV)				
	54.4	100	200	300	350
0	3.74^{1}	9.23^{1}	2.07^{2}	3.23^{2}	3.71^{2}
2	3.31^{1}	6.29^{1}	7.06^{1}	5.90^{1}	5.27^{1}
4	2.41^{1}	3.03^{1}	2.07^{1}	1.39^{1}	1.16^{1}
6	1.60^{1}	1.46^{1}	7.72	4.47	3.55
8	1.02^{1}	7.44	3.20	1.59	1.19
10	6.51	3.95	1.38	5.89^{-1}	4.13^{-1}
12	4.14	2.16	6.09^{-1}	2.21^{-1}	1.45^{-1}
14	2.64	1.20	2.71^{-1}	8.48^{-2}	5.27^{-2}
16	1.69	6.68^{-1}	1.22^{-1}	3.34^{-2}	1.99^{-2}
18	1.09	3.73^{-1}	5.63^{-2}	1.37^{-2}	7.99^{-3}
20	7.02^{-1}	2.09^{-1}	2.68^{-2}	6.03^{-3}	3.49^{-3}
25	2.48^{-1}	5.39^{-2}	5.67^{-3}	1.37^{-3}	8.19^{-4}
30	9.89^{-2}	1.90^{-2}	2.18^{-3}	6.01^{-4}	3.60^{-4}
35	4.97^{-2}	9.64^{-3}	1.21^{-3}	3.51^{-4}	2.11^{-4}
40	3.15^{-2}	6.06^{-3}	7.67^{-4}	2.21^{-4}	1.36^{-4}
45	2.22^{-2}	4.14^{-3}	5.21^{-4}	1.53^{-4}	8.76^{-5}
50	1.63^{-2}	2.96^{-3}	3.73^{-4}	1.11^{-4}	7.08^{-5}
60	9.59^{-3}	1.54^{-3}	2.14^{-4}	6.37^{-5}	3.96^{-5}
75	4.69^{-3}	7.21^{-4}	1.11^{-4}	3.51^{-5}	2.42^{-5}
90	2.57^{-3}	4.38^{-4}	7.14^{-5}	2.27^{-5}	1.57^{-5}
110	1.27^{-3}	2.73^{-4}	4.61^{-5}	1.54^{-5}	1.03^{-5}
120	1.01^{-3}	2.13^{-4}	3.87^{-5}	1.34^{-5}	8.1^{-6}
140	8.10^{-4}	1.43^{-4}	2.90^{-5}	1.04^{-5}	—
160	—	1.06^{-4}	2.48^{-5}	8.87^{-6}	—
180	—	8.96^{-5}	2.33^{-5}	8.33^{-6}	—

Summed 2s+2p cross sections are shown in figure 12. The experimental data here are those of Williams and Willis (1975), the error bars representing two standard deviations. The measurements at 100 and 300 eV do not agree with any of the theories beyond 30 and 60° respectively. Even though the thoretical curves are by no means in perfect accord this theoretical consensus strongly suggests that there is something wrong with the measurements in these regions. If the present cross sections are right then the experiment is in even greater error, since only at 20° does the present work agree with the data at 100 and 200 eV within the quoted error bars. It is noteworthy that the three-state close-coupling calculation seems to provide an (approximate) upper bound to the theoretical estimates of the 2s+2p cross section.

3.2.4. Integrated cross sections. Integrated 2p cross sections are given in table 12. Two sets of experimental data are shown. The first is the single absolute measurement of Williams (1981) at 54.4 eV. The second set is obtained by combining the relative data of Long *et al* (1968) with the Lyman-α polarisation measurements of Ott *et al* (1970), in the manner described by Kingston and Walters (1980), and normalising the result to our present theory at 200 eV.

It is seen from the table that the cross sections of Long *et al* are in very good agreement with our calculations while both are markedly different from the absolute measurement of Williams at 54.4 eV. The absolute measurement is supported by the

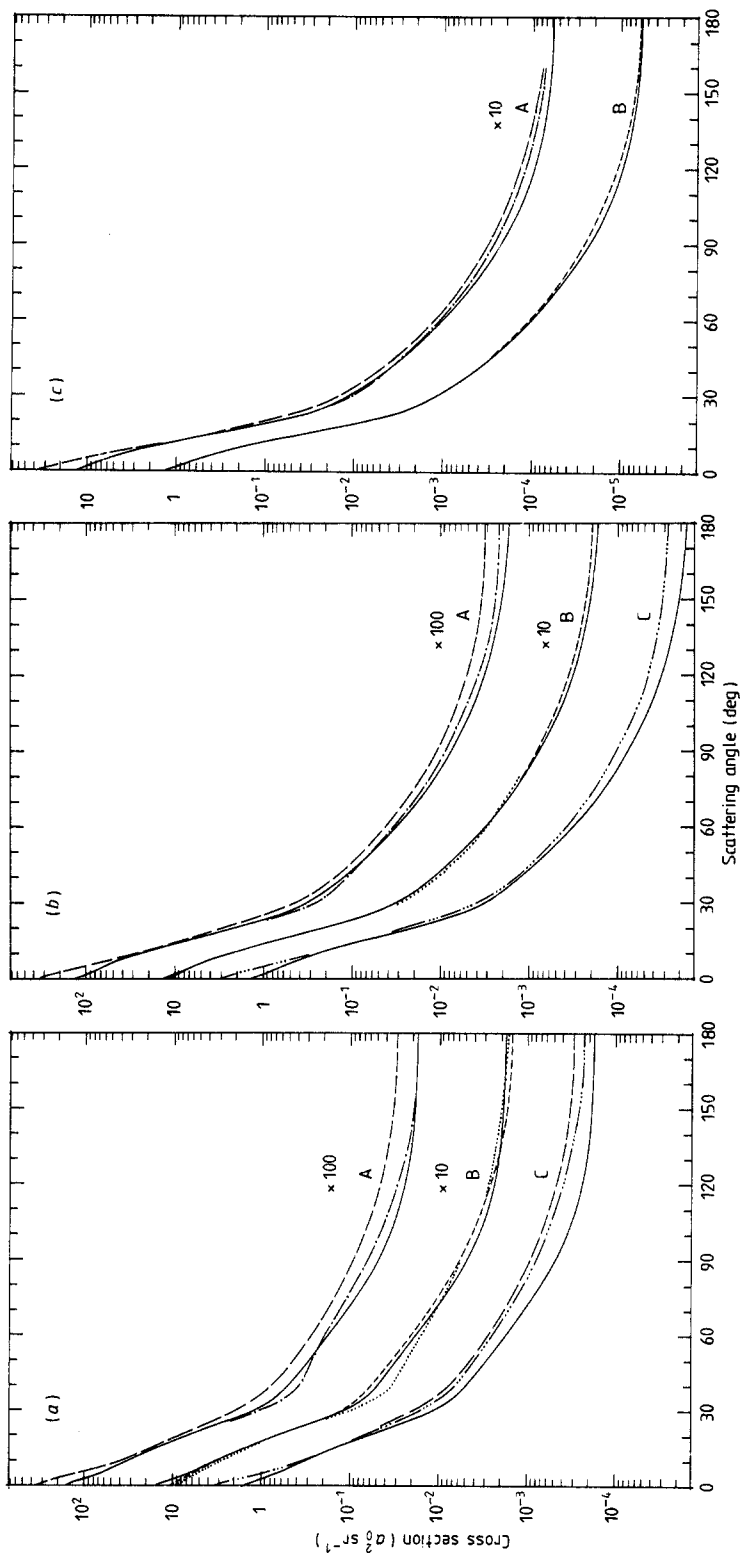

Figure 10. Differential cross sections for $e^- + H(1s) \rightarrow e^- + H(2s)$ at (*a*) 100 eV, (*b*) 200 eV, (*c*) 300 eV. The present results (——) are compared with A, the 1s–2s–2p close-coupling approximation of Kingston *et al* (1976) (——) and the DWSBA of Kingston and Walters (1980) (— · —), B, the UEBS of Byron *et al* (1985) (- - - -) and the SOPM of Bransden *et al* (1982) (· · · ·), and C, the 1s–2s–2p close-coupling approximation of Kingston *et al* (1976) (— —) and the CCOM of McCarthy and Stelbovics (1983a) (— · · · —).

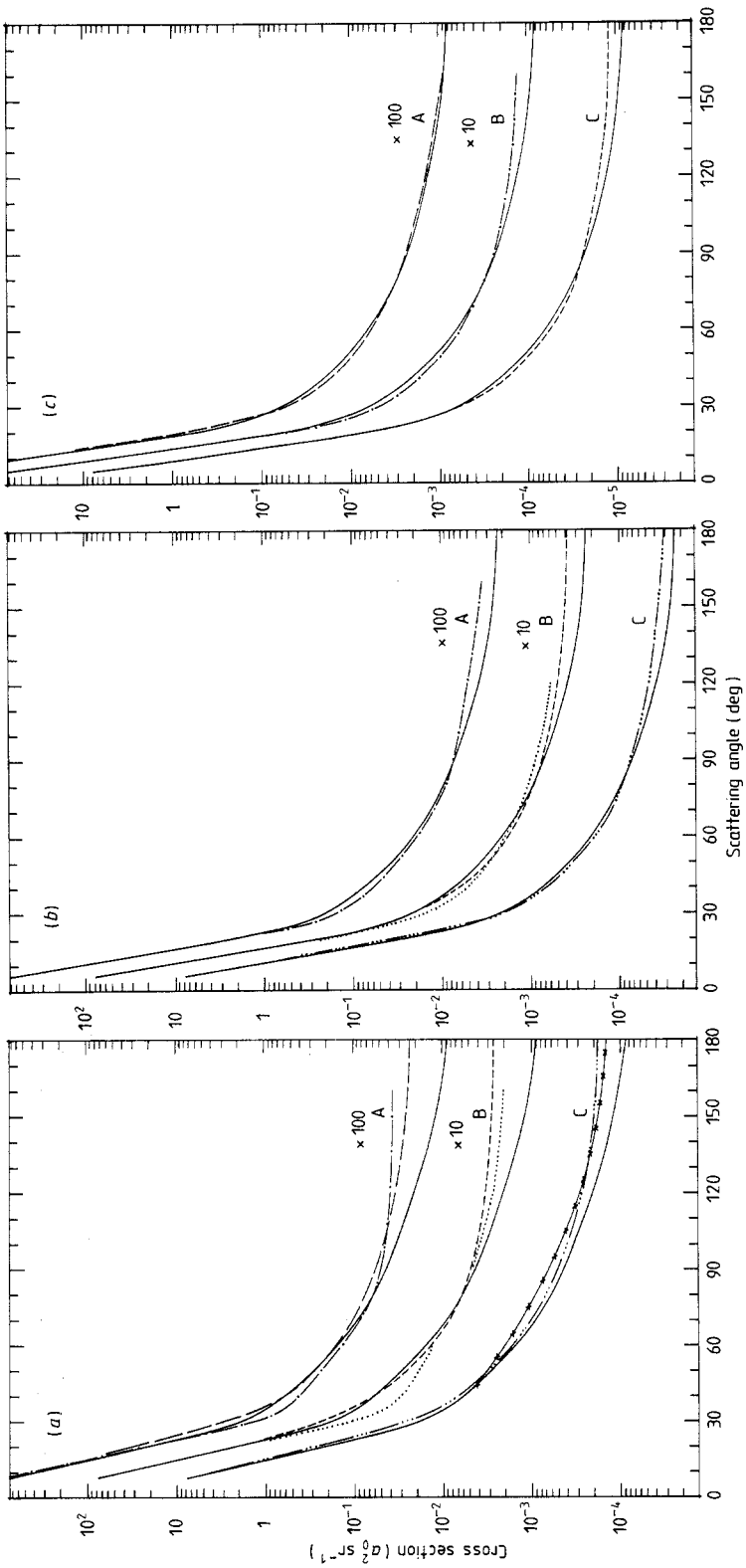

Figure 11. Differential cross sections for $e^- + H(1s) \rightarrow e^- + H(2p)$ at (*a*) 100 eV, (*b*) 200 eV, (*c*) 300 eV. ——, present results; — —, 1s–2s–2p close-coupling approximation of Kingston *et al* (1976); — · — · —, DWSBA of Kingston and Walters (1980); - - -, UEBS of Byron *et al* (1985); · · ·, SOPM of Bransden *et al* (1982); — · · · —, CCOM of McCarthy and Stelbovics (1983a); ✶✶, ESOT of Madison *et al* (1985).

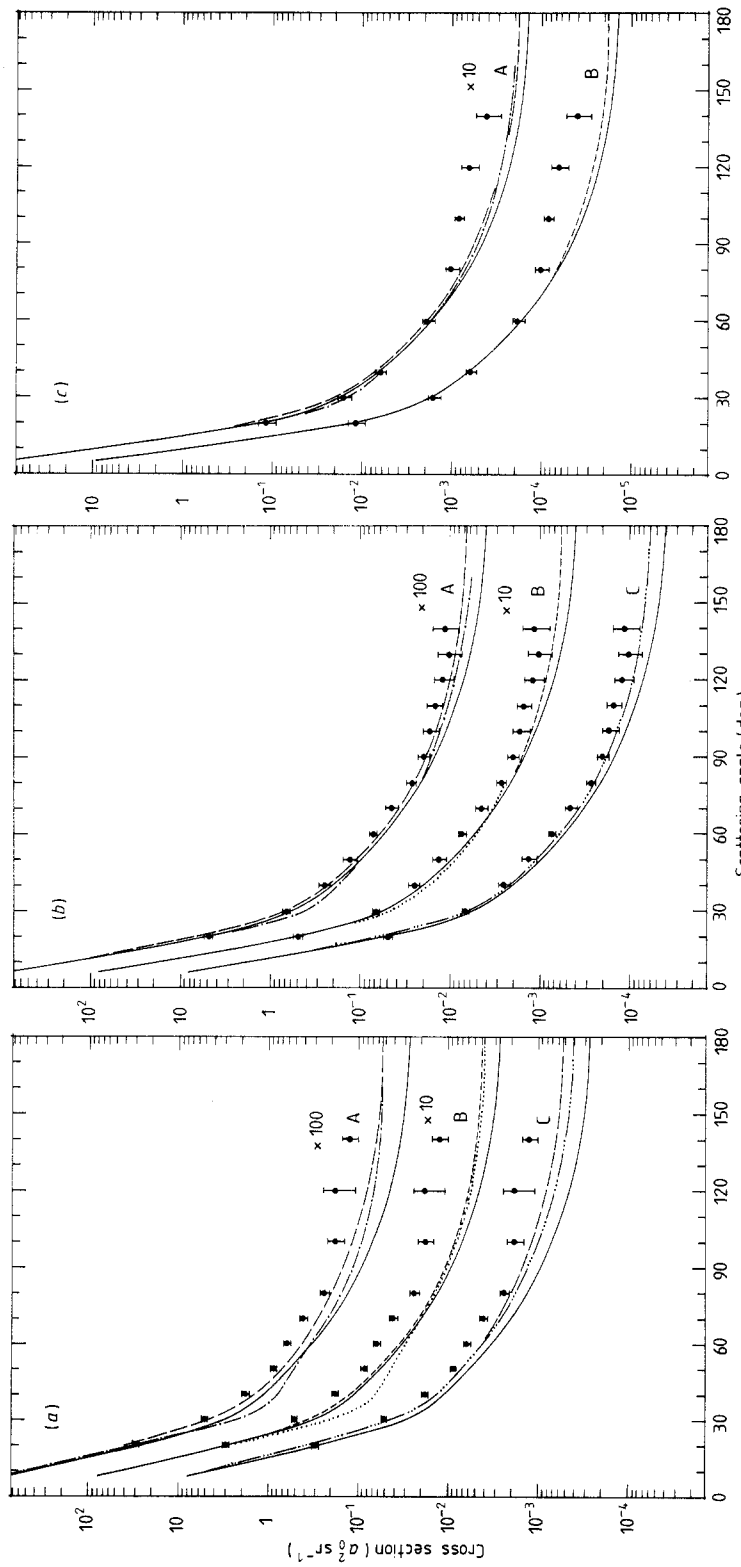

Figure 12. Differential cross sections for $e^- + H(1s) \rightarrow e^- + H(2s+2p)$ at (*a*) 100 eV, (*b*) 200 eV, (*c*) 300 eV. The present results (——) and the experimental data of Williams and Willis (1975) (●) are compared with A, the 1s–2s–2p close-coupling approximation of Kingston *et al* (1976) (— — —) and the DWSBA of Kingston and Walters (1980) (— · —), B, the UEBS of Byron *et al* (1985) (– – – –) and the SOPM of Bransden *et al* (1982) (· · · ·), and C, the 1s–2s–2p close-coupling approximation of Kingston *et al* (1976) (— — —) and the CCOM of McCarthy and Stelbovics (1983a) (— · · · —). The experimental error bars correspond to two standard deviations.

Table 12. Integrated cross sections for $e^- + H(1s) \rightarrow e^- + H(2p)$, in units of πa_0^2.

Energy (eV)	Expt[a]	Present	DWSBA[b]	UEBS[c]	SOPM[d]	CCOM[e]	CC3[f]
54.4	0.72 ± 0.03 0.89 ± 0.08 (W)	0.739	0.943	—	0.815	0.875	0.908
100	0.62 ± 0.03	0.638	0.709	0.60	0.672	0.662	0.681
200	0.45 ± 0.02	0.446	0.467	0.41	0.506	0.439	0.452
300	—	0.344	0.354	0.30	—	—	0.346
350	—	0.308	—	—	—	—	—

[a] Calculated from the measurements of Long *et al* (1968) using the Lyman-α polarisation fractions of Ott *et al* (1970) and normalised to the present results at 200 eV. At 54.4 eV the absolute measurement of Williams (1981) is labelled by (W). Errors correspond to two standard deviations.

[b] Distorted-wave second Born approximation of Kingston and Walters (1980).

[c] Unitarised eikonal-Born series of Byron *et al* (1985).

[d] Second-order potential method of Bransden *et al* (1982).

[e] Coupled-channels optical model: at 54.4 eV from Bransden *et al* (1984); at other energies from McCarthy and Stelbovics (1983a).

[f] Three-state 1s-2s-2p close-coupling of Kingston *et al* (1976).

DWSBA, SOPM (just), CCOM and CC3 approximations (no UEBS cross section is given at 54.4 eV). To make a fair comparison between the data of Long *et al* and the other theories it is necessary to normalise these data to the appropriate theory at 200 eV; when this is done it is found that the DWSBA, CCOM and CC3 results are in disagreement, predicting too large a cross section at 54.4 eV, while the SOPM and UEBS (at least down to 100 eV) are in accord.

The measurements of Long *et al* contain cascade contributions. At 200 eV the cascade effect is estimated to be about 2%. If the percentage cascade contribution does not change appreciably between 200 and 54.4 eV then normalisation to theory at 200 eV should produce a cross section which accurately reflects the behaviour of the true 2p curve. Since the cascade is merely 2% at 200 eV, the only significant way in which this effect can change with decreasing energy is to increase in size; this would produce an apparent 2p cross section which became too large with decreasing energy. It is interesting that those theories which disagree with the data of Long *et al* give a larger cross section than the measurements with decreasing energy, i.e., cascade effects cannot explain this difference.

Finally, we would observe that, compared with the other theories, the UEBS cross section looks slightly on the low side at the higher energies, while the SOPM result at 200 eV appears to be somewhat large.

Integrated 2s cross sections are shown in table 13. The 'experimental' values have been extracted from the data of Kauppila *et al* (1970)†. What Kauppila *et al* actually measure is Q_{2s} plus cascade contributions. It has been estimated (Hummer and Seaton 1961) that the cascade contributions can be reasonably represented by $0.23 Q_{3p}$ where Q_{3p} is the true $1s \rightarrow 3p$ cross section; this means that what Kauppila *et al* really measure is

$$Q_{2s} + 0.23 Q_{3p}. \tag{34}$$

† Cox and Smith (1971) have also reported similar measurements which, in the energy range of interest to us, support the data of Kauppila *et al*.

Table 13. Integrated cross sections for $e^- + H(1s) \rightarrow e^- + H(2s)$, in units of πa_0^2.

Energy (eV)	Expt[a]	Present	DWSBA[b]	UEBS[c]	SOPM[d]	CCOM[e]	CC3[f]
54.4	0.056 ± 0.005	0.0651	0.0595	—	0.0395	0.080	0.101
100	0.039 ± 0.004	0.0404	0.0427	0.038	0.0350	0.051	0.0582
200	0.025 ± 0.003	0.0250	0.0356	0.024	0.0239	0.029	0.0300
300	0.016 ± 0.002	0.0177	0.0181	0.018	—	—	0.0201
350	0.014 ± 0.002	0.0154	—	—	—	—	—

[a] Measurements of Kauppila *et al* (1970) with 1s → 3p cascade contribution subtracted as described in text. Errors correspond to two standard deviations.
[b] Distorted-wave second Born approximation of Kingston and Walters (1980). An inaccuracy in the numerical integrations of the 2s DWSBA cross section is corrected here.
[c] Unitarised eikonal-Born series of Byron *et al* (1985).
[d] Second-order potential method of Bransden *et al* (1982).
[e] Coupled-channels optical model: at 54.4 eV from Bransden *et al* (1984); at other energies from McCarthy and Stelbovics (1983a).
[f] Three-state 1s–2s–2p close coupling of Kingston *et al* (1976).

Previously, Kingston and Walters (1980) used the Glauber approximation for Q_{3p} to obtain the true 1s → 2s cross section from the data. Here we adopt a different procedure which we think is better. Writing (34) as

$$(1 + 0.23 Q_{3p}/Q_{2s}) Q_{2s} \tag{35}$$

we estimate the ratio Q_{3p}/Q_{2s} using the Glauber results of Tai *et al* (1970). The 'experimental' 2s cross section is then obtained by dividing the data of Kauppila *et al* by the factor $(1 + 0.23 Q_{3p}/Q_{2s})$.

The measurements of Kauppila *et al* were normalised by reference to the 2p data of Long *et al* (1968) which, in turn, were set on an absolute scale by comparison with the first Born approximation at 200 eV. In table 12 we have renormalised the Long *et al* cross sections to our 2p calculation at 200 eV; to be consistent with this, therefore, we must appropriately renormalise the data of Kauppila *et al*; this has been done in obtaining the numbers in table 13. The error bars quoted come from the experimental errors of Kauppila *et al* and represent two standard deviations; the errors do not include any estimate of the reliability of our procedure for extracting the cascade contribution.

The interesting thing about the 'experimental' results in table 13 is that at 54.4 eV they favour the present and DWSBA cross sections; these, it will be remembered, were in sharp disagreement with the experimental differential cross sections of Williams (1981) at this energy (figure 3). Those approximations which agreed with Williams' measurements, i.e., CCOM and CC3, are seen to be in substantial disagreement with the 'experimental' integral cross sections. Again, to be fair to other approximations we should normalise the measurements of Kauppila *et al* to the corresponding theoretical 2p cross section at 200 eV. From table 12 it is clear that this will not bring the 'experimental' 2s cross section into agreement with the CCOM and CC3 approximations at 54.4 eV.

The consistency of the agreement between the present calculation and the Long *et al* 2p cross section of table 12 and the admittedly tentative 'experimental' 2s cross section of table 13 is compelling; it is at odds with the impression gained from

comparisons with the differential cross sections of Williams (1981) and Williams and Willis (1975) (§§ 3.2.2 and 3.2.3). In view of the large differences which exist, a really accurate determination of just the integrated 2s and 2p cross sections in the energy range 54.4–300 eV would do much to clarify matters.

3.2.5. Polarisation of the Lyman-α radiation. The polarisation fractions P (see (29)) calculated in the present, DWSBA, CC3 and first Born approximations are compared with the experiment of Ott *et al* (1970) in table 14. The experiment measures Lyman-α polarisation irrespective of whether the 2p state is excited directly or populated by cascade; hopefully cascade effects are not too important in the energy range given in the table.

The present and DWSBA calculations agree with experiment within the quoted error bars. Interestingly though, the CC3 approximation at 54.4 eV is in disagreement.

Table 14. Polarisation fraction of Lyman-α radiation, P.

Energy (eV)	Expt[a]	Present	DWSBA[b]	CC3[c]	FBA[d]
54.4	$+0.12 \pm 0.02$	+0.110	+0.135	+0.0855	+0.088
100	$+0.05 \pm 0.02$	+0.039	+0.050	—	+0.027
200	0.0 ± 0.03	−0.015	−0.013	—	−0.023
300	-0.03 ± 0.04	−0.042	−0.040	—	−0.046
350	-0.03 ± 0.04	−0.054	—	—	−0.054

[a] Measurements of Ott *et al* (1970). Errors correspond to two standard deviations.
[b] Distorted-wave second Born approximation of Kingston and Walters (1980).
[c] Three-state 1s–2s–2p close-coupling of Burke *et al* (1963).
[d] First Born approximation.

3.2.6. Angular correlation parameters. Our λ, R and I parameters ((25)–(27)) are given in tables 15–17. In figures 13 and 14 the λ and R parameters at 100, 200 and 300 eV are compared with other calculations and with the experimental data of Hood *et al* (1979) and Slevin *et al* (1980). The experimental error bars correspond to two standard deviations. In the case of the Hood *et al* data we have estimated the errors ourselves, along the lines suggested by Slevin *et al* (1980); unfortunately these errors are so large as to make the data of Hood *et al* of little use to us. The measurements of Slevin *et al* are more discriminating but are not in agreement with our calculations, either for λ or R; in particular, the deep minimum in the experimental λ parameter at 10° is certainly not consistent with our results. Kingston *et al* (1982) have criticised the way in which the values of λ and R were deduced from the measured electron–photon coincidence curve.

The double minimum in the λ parameter at 54.4 eV (figure 7) is repeated at the higher energies. Figure 13 shows that the first minimum (near 15°) gets lower and moves to smaller angles with increasing energy. The large difference between the present and UEBS approximations at the second minimum (near 90°) persists at the higher energies; however, the ESOT of Madison *et al* (1985) comes closer to the present results at 100 eV.

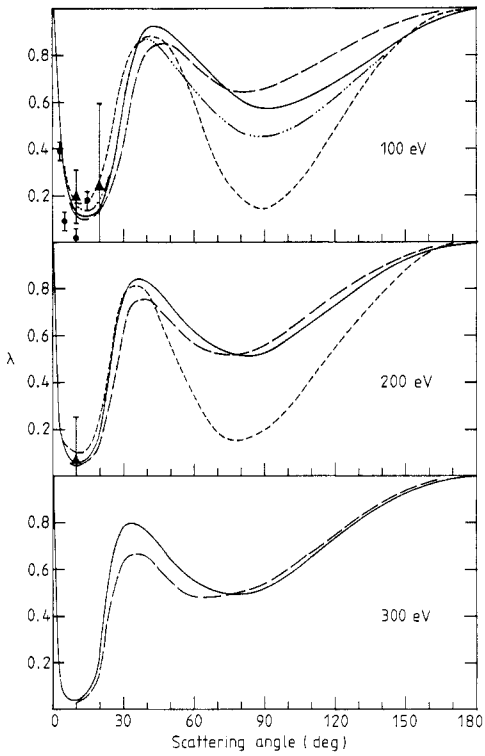

Figure 13. Angular correlation parameter λ at 100, 200 and 300 eV. ——, present results; — —, 1s-2s-2p close-coupling approximation of Kingston *et al* (1976); - - - -, UEBS of Byron *et al* (1985); — · · · —, ESOT of Madison *et al* (1985); ●, experimental data of Slevin *et al* (1980); ▲, experimental data of Hood *et al* (1979). The experimental errors bars correspond to two standard deviations.

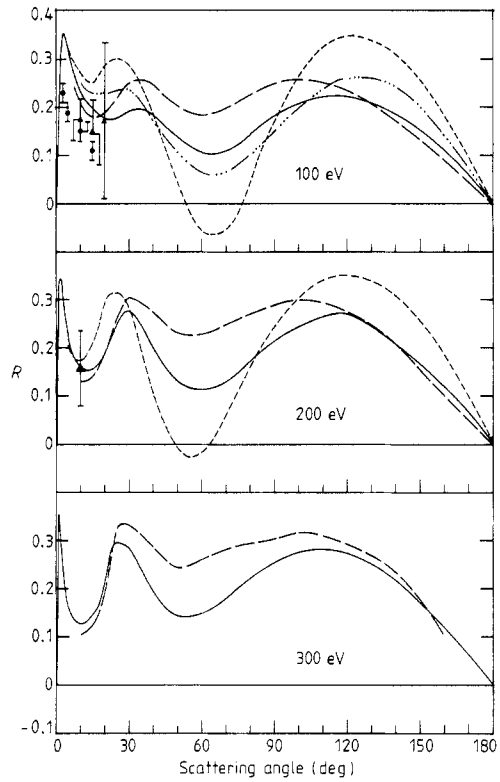

Figure 14. Angular correlation parameter R at 100, 200 and 300 eV. ——, present results; — —, 1s-2s-2p close-coupling approximation of Kingston *et al* (1976); - - - -, UEBS of Byron *et al* (1985); — · · · —, ESOT of Madison *et al* (1985); ●, experimental data of Slevin *et al* (1980); ▲, experimental data of Hood *et al* (1979). The experimental error bars correspond to two standard deviations.

All theories indicate that the R parameter has a third maximum near 30° at 100 eV (figure 14). With increasing energy this maximum becomes very pronounced.

Back *et al* (1984) have measured the λ and R parameters at 350 eV and at angles less than 10°. Their results and our present calculations are shown in figure 15. Our calculated values differ negligibly from the first Born approximation, i.e., the theory is dominated by the first Born term. This means that the theoretical predictions are on very firm ground indeed; the discrepancy with experiment seen in figure 15 is therefore serious. Back *et al* state that the angular acceptance of their electron analyser is $\pm\frac{1}{2}°$; the measured values of λ and R are thus averages over this angular range (Slevin *et al* 1982)†. Averaging the theoretical curves of figure 15 over $\pm\frac{1}{2}°$ makes very little change, i.e., angular resolution cannot explain the difference between theory and experiment.

† The electron-photon correlation function is linear in λ and R, see equation (1) of Slevin *et al* (1982).

Table 15. Present values of the angular correlation parameter λ. Powers of ten are denoted by a superscript.

Angle (deg)	Energy (eV)				
	54.4	100	200	300	350
0	1.0	1.0	1.0	1.0	1.0
2	0.902	0.711	0.377	0.211	0.162
4	0.702	0.391	0.147	0.747^{-1}	0.567^{-1}
6	0.521	0.237	0.859^{-1}	0.460^{-1}	0.367^{-1}
8	0.393	0.166	0.646^{-1}	0.384^{-1}	0.332^{-1}
10	0.310	0.133	0.581^{-1}	0.396^{-1}	0.373^{-1}
12	0.258	0.118	0.605^{-1}	0.480^{-1}	0.484^{-1}
14	0.227	0.112	0.716^{-1}	0.662^{-1}	0.701^{-1}
16	0.212	0.115	0.945^{-1}	0.101	0.110
18	0.210	0.127	0.135	0.164	0.182
20	0.220	0.153	0.200	0.269	0.294
25	0.306	0.315	0.493	0.621	0.627
30	0.488	0.593	0.763	0.787	0.761
35	0.717	0.825	0.839	0.792	0.742
40	0.879	0.916	0.829	0.758	0.723
45	0.952	0.924	0.787	0.703	0.638
50	0.974	0.891	0.723	0.640	0.608
60	0.955	0.797	0.621	0.555	0.491
75	0.848	0.645	0.525	0.488	0.495
90	0.716	0.573	0.524	0.517	0.548
110	0.611	0.628	0.657	0.657	0.644
120	0.619	0.685	0.727	0.735	0.708
140	0.747	0.810	0.874	0.871	—
160	—	0.933	0.968	0.965	—
180	—	1.0	1.0	1.0	—

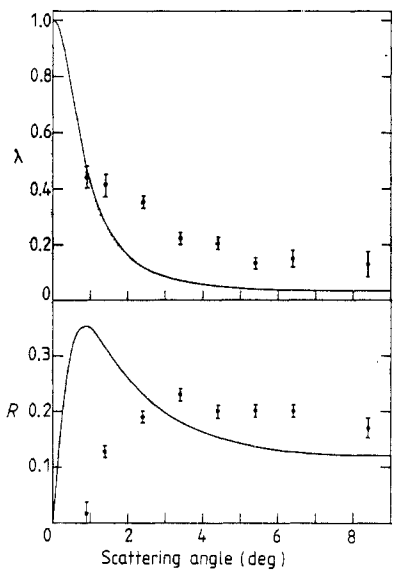

Figure 15. Angular correlation parameters λ and R at 350 eV. ——, present results; ⬢, experimental data of Back *et al* (1984). The error bars correspond to two standard deviations.

Table 16. Present values of the angular correlation parameter R. Powers of ten are denoted by a superscript.

Angle (deg)	Energy (eV)				
	54.4	100	200	300	350
0	0	0	0	0	0
2	0.209	0.320	0.343	0.288	0.260
4	0.322	0.346	0.250	0.185	0.163
6	0.351	0.300	0.197	0.146	0.131
8	0.341	0.261	0.170	0.131	0.121
10	0.320	0.234	0.157	0.127	0.122
12	0.298	0.217	0.152	0.130	0.129
14	0.277	0.204	0.153	0.139	0.141
16	0.260	0.193	0.159	0.153	0.160
18	0.246	0.184	0.171	0.176	0.190
20	0.233	0.177	0.188	0.210	0.232
25	0.205	0.178	0.250	0.296	0.312
30	0.183	0.189	0.274	0.285	0.297
35	0.166	0.195	0.246	0.242	0.254
40	0.150	0.182	0.198	0.192	0.210
45	0.129	0.159	0.158	0.162	0.174
50	0.105	0.139	0.128	0.144	0.177
60	0.468^{-1}	0.106	0.113	0.149	0.179
75	-0.649^{-2}	0.121	0.148	0.200	0.224
90	0.208^{-1}	0.183	0.216	0.254	0.255
110	0.146	0.222	0.263	0.280	0.300
120	0.197	0.222	0.267	0.272	0.297
140	0.148	0.186	0.206	0.218	—
160	—	0.109	0.118	0.123	—
180	—	0	0	0	—

The main purpose of the Back *et al* experiment, however, was to measure coherence between the 2s and 2p excitations. Their measurements yield two quantities

$$M_1+M_3=\frac{1.78\langle|f_s|^2\rangle+13.11\langle|f_0|^2\rangle+13.46\langle|f_1|^2\rangle+2.65\langle\mathrm{Re}(f_sf_0^*)\rangle}{10.91\langle|f_s|^2\rangle+14.03\langle|f_0|^2\rangle+16.00\langle|f_1|^2\rangle+0.16\langle\mathrm{Re}(f_sf_0^*)\rangle} \tag{36a}$$

$$M_2=\frac{1.50\langle|f_s|^2\rangle+0.06\langle|f_0|^2\rangle+0.25\langle|f_1|^2\rangle-0.58\langle\mathrm{Re}(f_sf_0^*)\rangle}{10.91\langle|f_s|^2\rangle+14.03\langle|f_0|^2\rangle+16.00\langle|f_1|^2\rangle+0.16\langle\mathrm{Re}(f_sf_0^*)\rangle}. \tag{36b}$$

Here $f_0^{\pm}$ and $f_1^{\pm}$ are the 2p amplitudes used in (26)-(28), $f_s^{\pm}$ is the $1s\rightarrow 2s$ amplitude and $\langle\ \rangle$ is the spin average defined in (28). Although there are actually three parameters, two of them, M_1 and M_3, cannot be separated. For this part of the experiment the electron detector had an angular acceptance of 7°; near the forward direction this was effectively increased to 8° due to the presence of the electric field which was used to Stark-mix the $n=2$ states; this field also caused the incident electron energy to be uncertain by about ±12 eV.

The experimental values of M_1+M_3 and M_2 are plotted in figure 16 as a function of the mean scattering angle (see above); here they are compared with the present calculation. Unlike the experiment, the theoretical numbers correspond to the precise energy of 350 eV and to the precise scattering angle shown; to make a proper comparison with experiment the theoretical values should really be averaged over the angular

Table 17. Present values of the angular correlation parameter I. Powers of ten are denoted by a superscript.

Angle (deg)	Energy (eV)				
	54.4	100	200	300	350
0	0.0	0.0	0.0	0.0	0.0
2	-0.134^{-1}	-0.832^{-2}	-0.625^{-2}	-0.540^{-2}	-0.589^{-2}
4	-0.265^{-1}	-0.169^{-1}	-0.145^{-1}	-0.130^{-1}	-0.137^{-1}
6	-0.394^{-1}	-0.263^{-1}	-0.245^{-1}	-0.226^{-1}	-0.237^{-1}
8	-0.525^{-1}	-0.375^{-1}	-0.369^{-1}	-0.353^{-1}	-0.369^{-1}
10	-0.665^{-1}	-0.512^{-1}	-0.527^{-1}	-0.526^{-1}	-0.550^{-1}
12	-0.822^{-1}	-0.681^{-1}	-0.730^{-1}	-0.762^{-1}	-0.795^{-1}
14	−0.100	-0.887^{-1}	-0.989^{-1}	−0.108	−0.112
16	−0.121	−0.113	−0.131	−0.147	−0.152
18	−0.145	−0.143	−0.169	−0.193	−0.194
20	−0.171	−0.177	−0.208	−0.230	−0.222
25	−0.243	−0.264	−0.243	−0.166	−0.133
30	−0.289	−0.275	−0.105	0.337^{-1}	0.397^{-1}
35	−0.260	−0.165	0.620^{-1}	0.150	0.175
40	−0.167	-0.261^{-1}	0.172	0.233	0.235
45	-0.700^{-1}	0.808^{-1}	0.240	0.279	0.292
50	0.866^{-2}	0.163	0.288	0.307	0.296
60	0.127	0.259	0.323	0.318	0.305
75	0.244	0.311	0.320	0.291	0.273
90	0.314	0.296	0.279	0.246	0.242
110	0.309	0.260	0.208	0.185	0.157
120	0.276	0.242	0.167	0.153	0.124
140	0.254	0.206	0.113	0.929^{-1}	—
160	—	0.139	0.395^{-1}	0.397^{-1}	—
180	—	0.0	0.0	0.0	—

resolution of the electron detector and over the energy uncertainty in the incident beam. Despite these differences, the agreement between theory and experiment seen in figure 16 is encouraging.

It is of interest to ask to what extent the parameters M_1+M_3 and M_2 reveal the presence of the 2s state. In figure 16 we also show our results when the 2s excitation is 'switched off', i.e., $f_s^{\pm}$ is set to zero in (36). We see that beyond 2° the switched-off values are noticeably different from the original numbers, and very flat—obviously

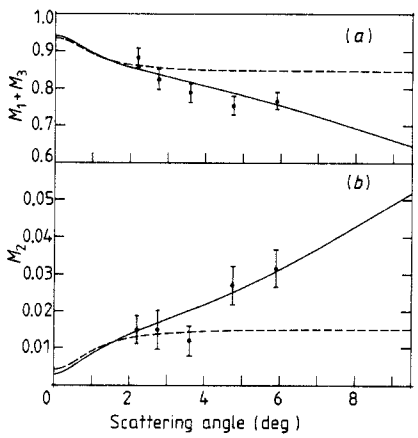

Figure 16. Variation with angle of (*a*) M_1+M_3, (*b*) M_2. ——, present results; - - - -, present results when 2s contribution is set to zero; ⧫, experimental data of Back *et al* (1984). The error bars correspond to two standard deviations.

there is good sensitivity to the 2s state here. That the experiment seems to be clearly showing the presence of the 2s state is pleasing.

Finally, we would remind the reader that approximation (17) has been used for both the 2s and 2p calculations at 350 eV, i.e., we have not gone as far as our best approximation (18). We have calculated the parameters (36) in the angular range 0–10° at 300 eV using both approximations (17) and (18) and have found negligible difference. We conclude that (17) is as good as (18) for the comparisons of figure 16.

4. Conclusions

The situation for elastic scattering is quite satisfactory. At 200 and 300 eV there is good reason to believe that the present differential cross sections are accurate to better than 5% at any angle. We think this is probably also the case at 100 eV, although we have no direct evidence. The quality of the theory is now better than that of the experiment.

The $1s \rightarrow 2s$ and $1s \rightarrow 2p$ transitions are more problematical. Here the various theoretical approximations are somewhat at odds with one another. However, there are areas where the theories are unanimously in disagreement with experiment, for example, the $1s \rightarrow 2s + 2p$ excitation at 100 and 300 eV (figures 12(a) and 12(c)). Here it is fair to suggest that it is experiment which is at fault rather than theory. A comparison of figures 1 and 12(a) shows that this is an advance upon the theoretical position of a few years ago when it was impossible to draw any definite conclusions about the experimental data. If the present calculations are accurate then the experimental differential cross sections for the 2s and 2p transitions are even more in error than the aggregate of theoretical approximations would suggest. Most striking is the difference between the experimental results for differential and integral cross sections. The former are not generally in good agreement with the present work, but the latter usually are (tables 12 and 13); in the future it will be interesting to see which are right. Although the theoretical picture is still unsatisfactory, it has been refined to a point where the onus is now moving on to experiment to correct and improve upon the measurements which currently exist.

As far as the angular correlation parameters for the $1s \rightarrow 2p$ excitation are concerned, it is fair to say that the present results are in reasonable agreement with the main experiment at 54.4 eV in the angular range up to 70° (figures 7 and 8). However, the situation beyond 70° is still confused; this is especially true of the R parameter where all theories insist upon a positive value at large angles contrary to experiment (figure 8).

Although we have made a wide-ranging comparison with other theoretical work, we are of the opinion that the present calculations are on the firmest ground (see § 1). That is not to say that the present work cannot be improved. There are four obvious ways in which changes could be made: (i) keeping the closed channels when solving (15) using the improved pseudostates; (ii) using, rather than approximation (17), the exact solution of (15) including exchange when the improved pseudostates are used; (iii) using of the improved pseudostates at 54.4 eV; (iv) adopting of a better approximation than DWSBA for the contribution of target states with angular momenta greater than or equal to three. While it would be nice to implement all of these suggestions, it is our feeling that they will probably not alter the results presented here very much.

Acknowledgments

This work was supported by the Science and Engineering Research Council of the United Kingdom (SERC). Most of the calculations were carried out on the Cray-1S

computer at the University of London Computer Centre under grants provided by SERC and the Department of Education for Northern Ireland.

References

Back C G, Watkin S, Eminyan M, Rubin K, Slevin J and Woolsey J M 1984 *J. Phys. B: At. Mol. Phys.* **17** 2695-706
Bransden B H and Dewangan D P 1979 *J. Phys. B: At. Mol. Phys.* **12** 1377-89
Bransden B H, McCarthy I E and Stelbovics A T 1984 *J. Phys. B: At. Mol. Phys.* **17** 4543-7
Bransden B H, Scott T, Shingal R and Roychoudhury R K 1982 *J. Phys. B: At. Mol. Phys.* **15** 4605-16
Buckley B D and Walters H R J 1975 *J. Phys. B: At. Mol. Phys.* **8** 1693-715
Burke P G, Schey H M and Smith K 1963 *Phys. Rev.* **129** 1258-74
Byron F W Jr and Joachain C J 1973 *Phys. Rev.* A **8** 1267-82
—— 1977 *J. Phys. B: At. Mol. Phys.* **10** 207-26
—— 1981 *J. Phys. B: At. Mol. Phys.* **14** 2429-48
Byron F W Jr, Joachain C J and Potvliege R M 1981 *J. Phys. B: At. Mol. Phys.* **14** L609-15
—— 1982 *J. Phys. B: At. Mol. Phys.* **15** 3915-43
—— 1985 *J. Phys. B: At. Mol. Phys.* **18** 1637-60
Byron F W Jr and Latour L J Jr 1976 *Phys. Rev.* A **13** 649-64
Callaway J, McDowell M R C and Morgan L A 1976 *J. Phys. B: At. Mol. Phys.* **9** 2043-51
Cox D M and Smith S J 1971 *Proc. 7th Int. Conf. on Physics of Electronic and Atomic Collisions* (Amsterdam: North-Holland) Abstracts pp 707-8
Dewangan D P and Walters H R J 1977 *J. Phys. B: At. Mol. Phys.* **10** 637-61
Edmunds P W, McDowell M R C and Morgan L A 1983 *J. Phys. B: At. Mol. Phys.* **16** 2553-66
Fon W C, Berrington K A, Burke P G and Kingston A E 1981 *J. Phys. B: At. Mol. Phys.* **14** 1041-51
Gien T T 1979 *Phys. Rev.* A **20** 1457-67
de Heer F J, McDowell M R C and Wagenaar R W 1977 *J. Phys. B: At. Mol. Phys.* **10** 1945-53
Hood S T, Weigold E and Dixon A J 1979 *J. Phys. B: At. Mol. Phys.* **12** 631-48
Hummer D G and Seaton M J 1961 *Phys. Rev. Lett.* **6** 471-2
Kauppila W E, Ott W R and Fite W L 1970 *Phys. Rev.* A **1** 1099-108
Kingston A E, Fon W C and Burke P G 1976 *J. Phys. B: At. Mol. Phys.* **9** 605-18
Kingston A E, Liew Y C and Burke P G 1982 *J. Phys. B: At. Mol. Phys.* **15** 2755-66
Kingston A E and Walters H R J 1980 *J. Phys. B: At. Mol. Phys.* **13** 4633-62
—— 1982 *Commun. At. Mol. Phys.* **11** 177-91
Lloyd C R, Teubner P J O, Weigold E and Lewis B R 1974 *Phys. Rev.* A **10** 175-81
Long R L, Cox D M and Smith S J 1968 *J. Res. NBS* A **72** 521-35
McCarthy I E, Saha B C and Stelbovics A T 1981 *J. Phys. B: At. Mol. Phys.* **14** 2871-93
—— 1982 *Phys. Rev.* A **25** 268-70
McCarthy I E and Stelbovics A T 1983a *J. Phys. B: At. Mol. Phys.* **16** 1233-45
—— 1983b *Phys. Rev.* A **28** 2693-707
Madison D H, Hughes J A and McGinness D S 1985 *J. Phys. B: At. Mol. Phys.* **18** 2737-61
Morgan L A 1982 *J. Phys. B: At. Mol. Phys.* **15** 4247-57
Morgan L A and McDowell M R C 1975 *J. Phys. B: At. Mol. Phys.* **8** 1073-81
Ott W R, Kauppila W E and Fite W L 1970 *Phys. Rev.* A **1** 1089-98
Percival I C and Seaton M J 1958 *Phil. Trans. R. Soc.* A **251** 113-38
Scott T and Bransden B H 1981 *J. Phys. B: At. Mol. Phys.* **14** 2277-89
Slevin J 1984 *Rep. Prog. Phys.* **47** 463-511
Slevin J, Eminyan M, Woolsey J M, Vassilev G and Porter H Q 1980 *J. Phys. B: At. Mol. Phys.* **13** L341-5
Slevin J, Eminyan M, Woolsey J M, Vassilev G, Porter H Q, Back C G and Watkin S 1982 *Phys. Rev.* A **26** 1344-9
Tai H, Bassel R H and Gerjuoy E 1970 *Phys. Rev.* A **1** 1819-35
Walters H R J 1981 *J. Phys. B: At. Mol. Phys.* **14** 3499-511
—— 1984 *Phys. Rep.* **116** 1-102
Weigold E, Frost L and Nygaard K J 1980 *Phys. Rev.* A **21** 1950-4
Williams J F 1975 *J. Phys. B: At. Mol. Phys.* **8** 2191-9
—— 1981 *J. Phys. B: At. Mol. Phys.* **14** 1197-217
Williams J F and Willis B A 1975 *J. Phys. B: At. Mol. Phys.* **8** 1641-69
van Wingerden B, Weigold E, de Heer F J and Nygaard K J 1977 *J. Phys. B: At. Mol. Phys.* **10** 1345-62
Winters K H, Clark C D, Bransden B H and Coleman J P 1974 *J. Phys. B: At. Mol. Phys.* **7** 788-98